# LUND UNIVERSITY

**Predictive Control of Diabetic Glycemia**

Stemmann, Meike

2013

[Link to publication](Link to publication)

*Total number of authors:*
1

# Predictive Control of Diabetic Glycemia

Meike Stemmann

Department of Automatic Control
Lund University
Lund, March 2013

# Abstract

Diabetes Mellitus is a chronic disease, where the blood glucose concentration of the patient is elevated. This is either because of missing insulin production due to failure of the $\beta$-cells in the pancreas (Type 1) or because of reduced sensitivity of the cells in the body to insulin (Type 2). The therapy for Type 1 diabetic patients usually consists of insulin injections to substitute for the missing insulin. The decision about the amount of insulin to be taken has to be made by the patient, based on empirically developed rules of thumb.

To help the patient with this task, advanced mathematical algorithms were used in this thesis to determine intakes of insulin and counteracting glucose that can bring the blood glucose concentration back to normoglycemia. The focus in this work was to determine insulin and glucose intakes around mealtimes. These algorithms used optimization methods together with predictions of the blood glucose concentration and mathematical models describing the patient dynamics to determine the insulin and glucose doses. For evaluation, the control algorithms were tested in-silico using a virtual patient and are compared to a simple bolus calculator from the literature. The aim was to increase the time spent in the safe range of blood glucose values of $70 - 180$ [mg/dL].

# Acknowledgments

First of all, I would like to thank my first supervisor Rolf Johansson for giving me the opportunity to come to do my Ph.D. thesis here in Lund and for his supervision and guidance. Furthermore, I would like to thank my second supervisor Anders Rantzer for his help and valuable feedback.

Thanks also to my DIAdvisor$^{TM}$ colleagues here in Lund, Marzia Cescon and Fredrik Ståhl for their collaboration, support and encouragement. Many thanks as well to Rolf Johansson, Anders Rantzer, Per Hagander, Fredrik Ståhl and Marzia Cescon for taking time to proofread my thesis.

This work was supported by the European FP7 IST-216592 Project DIAdvisor$^{TM}$. I would like to thank everybody that took part in the DIAdvisor$^{TM}$ project. It was a very interesting experience to gain insight into a field that was very new to me when I started my Ph.D.

I am very grateful to everybody at the Department of Automatic Control in Lund for creating such a great and pleasant working environment. With all the courses and workshops offered one gets a great chance to grow intellectually during the time as a Ph.D. student, and I have learnt a lot during my time here.

I would also like to thank the administrative staff Eva Westin, Lizette Borgeram, Ingrid Nilsson, Monika Rasmusson, Eva Schildt and Britt-Marie Mårtensson for all their support. Organizational and administrative matters always run very smoothly.

Many thanks go to Alina for our occasional third coffee break of the day, and for a lot of encouragement. Thanks a lot also to Marzia for support and discussions during the time we have been sharing office. Fur-

thermore, I would like to thank Martin, Andreas and Olof for the time that we shared the office during my first two years in Lund.

Moreover, I will always be grateful to my family, for making it possible that I could come to Lund in the first place and for always supporting me. Special thanks I owe to my fiancé Roger for his understanding, patience and all the encouragement and support he gave me.

# Contents

*Contents*

# List of Symbols

| | |
|---|---|
| BG | blood glucose |
| MDI | multiple daily injections of insulin |
| MPC | Model Predictive Control |
| PID | proportional-integral-derivative control |
| T1DM | Diabetes Mellitus Type 1 |
| T2DM | Diabetes Mellitus Type 2 |
| NPH | neutral protamine Hagedorn insulin |
| IOB | insulin on board |
| $U_{id}(t)$ | insulin-dependent glucose utilization |
| $U_{ii}(t)$ | insulin-independent glucose utilization |
| $E(t)$ | renal excretion |
| $G(t)$ | plasma glucose concentration of the virtual patient |
| $G_p(t)$ | glucose masses in plasma and rapidly equilibrating tissues |
| $G_t(t)$ | glucose masses in slowly equilibrating tissues |
| $R_a(t)$ | glucose rate of appearance in plasma |
| $V_g$ | distribution volume of glucose |
| $\dot{G}_{\text{EGP}}(t)$ | endogenous glucose production |

*List of Symbols*

$k_1, k_2$      parameters of the glucose system in the virtual patient

$I(t)$      plasma insulin concentration

$I_l(t)$      insulin masses in the liver

$I_p(t)$      insulin masses in plasma

$Q_{gut}(t)$      glucose mass in the intestine

$Q_{sto1}(t)$      amount of glucose in the stomach, solid phase

$Q_{sto2}(t)$      amount of glucose in the stomach, liquid phase

$Q_{sto}(t)$      amount of glucose in the stomach

$S(t)$      insulin secretion

$V_i$      distribution volume of insulin

$W_{\text{body}}$      body weight

$d(t)$      rate of ingested glucose

$f$      fraction of intestinal glucose absorption that appears in the plasma

$k_{abs}$      rate constant of intestinal absorption of glucose

$k_{e2}$      threshold of glucose in blood for renal excretion of insulin

$k_{gri}$      rate of grinding of glucose

$k_{gut}$      rate constant of gastric emptying

$m_1, m_2$      rate parameters

$m_3, m_4$      rate parameters

$I_d$      delayed insulin signal

$\bar{t}_s, \bar{t}_f$      initial and final time of the last glucose ingestion

$a_v, b_v$      model parameter for the gastro-intestinal tract of the virtual patient

$k_{ins}$      a parameter describing the delay between the insulin signal and insulin action

$k_{min}, k_{max}$  model parameter for the gastro-intestinal tract of the virtual patient

$k_{p1}$  the extrapolated $\dot{G}_{\text{EGP}}(t)$ at zero glucose

$k_{p2}$  liver glucose effectiveness

$k_{p3}$  a parameter that influences the amplitude of insulin action on the liver

$I_b$  basal insulin

$K_m, V_{m0}, V_{mx}$  model parameters for the muscle and adipose tissues of the virtual patient

$X(t)$  remote insulin

$p_{2U}$  rate constant of insulin action on peripheral glucose utilization

$I_{sc1}$  amount of nonmonomeric insulin in the subcutaneous space

$I_{sc2}$  amount of monomeric insulin in the subcutaneous space

$R_{Inf}(t)$  infusion rate of exogenous insulin

$k_d$  rate constant of insulin dissociation

$k_{a1}, k_{a2}$  rate constants connected to nonmonomeric and monomeric insulin absorption

$A, B, K, C$  matrices representing patient dynamics in a state-space model

$\bar{y}_{BG}$  mean value of the blood glucose concentration at the output of the virtual patient

$u$  vector representing insulin and glucose rate of appearance inputs

$x$  states of the patient model in state-space form

$y$  a blood glucose concentration

$y_{BG}$  blood glucose concentration at the output of the virtual patient

$y_M$  BG at the output of the estimated state-space model

$H_p$  prediction horizon

$p$  number of time steps into the future

## List of Symbols

| | |
|---|---|
| $\hat{y}_{H_p}$ | vector collecting future predicted BG concentrations, for the next $H_p$ time steps |
| $h$ | sampling time |
| $k$ | sampling instant |
| $N$ | number of data points measured |
| $a_g$ | dose size of a glucose intake |
| $a_i$ | dose size of an insulin intake |
| $c_{\text{offset},BG}$ | initial offset in the output data of the virtual patient |
| $k_g$ | time index for glucose intake ( $t_g = h \cdot k_g$) |
| $k_i$ | time index for glucose intake ( $t_i = h \cdot k_i$) |
| $t_g$ | time for glucose intake in [min] |
| $t_i$ | time for insulin intake in [min] |
| $y_{h,g}(k; k_g, a_g)$ | controller patient model: effect of a glucose intake of size $a_g$ at time $k_g$ on the blood glucose concentration |
| $y_{h,i}(k; k_i, a_i)$ | controller patient model: effect of an insulin intake of size $a_i$ at time $k_i$ on the blood glucose concentration |
| $J$ | Asymmetric cost function |
| $L$ | integrant of the cost function |
| $\hat{y}$ | blood glucose concentration predicted by the prediction algorithm |
| $k_0$ | time instant the optimization algorithm is called |
| $\bar{u}_{RA}(k)$ | insulin and glucose rates of appearance after a meal for the selection-based controller |
| $\tilde{u}_{RA}(k)$ | insulin and glucose rates of appearance of doses suggested by the selection-based controller |
| $u_{RA}(k)$ | vector with glucose and insulin rate of appearance as input to the state-space patient model used in the selection-based controller |

| | |
|---|---|
| $u_{RA}^{(1)}(k)$ | glucose rate of appearance as input to the state-space patient model used in the selection-based controller |
| $u_{RA}^{(1)}(k)$ | insulin rate of appearance as input to the state-space patient model used in the selection-based controller |
| $y_s(k+p)$ | blood glucose prediction for the selection-based controller, including meals and dose intakes from the controller |
| $\mathcal{Y}_{s,H_p}$ | blood glucose concentration predicted over the prediction horizon for the selection-based controller |
| $\tilde{\mathcal{U}}_{1,H_p}, \tilde{\mathcal{U}}_{2,H_p}$ | rates of appearance of glucose and insulin doses to be suggested by the selection-based control algorithm over the prediction horizon |
| $M$ | amount of carbohydrates in a meal |
| $c_{\text{TDD}}$ | total daily dose of insulin |
| $c_{\text{ISF}}$ | insulin sensitivity factor |
| $c_{\text{ITC}}$ | insulin-to-carbohydrate ratio |
| $y_{\text{r}}$ | reference blood glucose concentration for the bolus calculator |
| $\text{T}_{\text{safe}}[\%]$ | percent of time spent in normal BG range of $70 - 180$ [mg/dL] |
| $r$ | risk function according to Kovatchev |
| HBGI | high BG index |
| LBGI | low BG index |
| $G_\sum$ | total amount of glucose advised per day |
| $I_\sum$ | total amount of insulin units advised per day |

# 1

# Introduction

*Diabetes Mellitus* is a chronic disease caused either by the inability of the body to produce insulin (Type 1) or because the cells in the body do not respond to the effect of insulin (Type 2). In type 1 diabetes, a failure of the $\beta$-cells in the pancreas caused by, e.g., injuries, infections or autoimmune disorders, leads to a lack of insulin secretion. This lack of insulin secretion leads to chronically elevated blood glucose levels, which results in complications affecting, for example, the heart, liver, kidneys or nerves [1].

Diabetes is one of the leading causes of blindness, amputation and kidney failure in the world [2]. There are 331 million people with diabetes worldwide and more than 55 million in Europe. The number of people with diabetes is projected to increase from 8.3 % of the world population in 2012 to 9.9 % of the world population in 2030 [3]. Although $85 - 95$ % of adult people with diabetes are suffering from type 2 diabetes, the number of people with type 1 diabetes is increasing around the world each year. Furthermore, the majority of young people suffering from diabetes have type 1 diabetes [4].

For treatment, patients with type 1 diabetes have to substitute the missing insulin by administrating insulin externally. This is done either through multiple insulin injections during the day (MDI) or by continuous insulin infusion subcutaneously with a pump. Patients treated with multiple daily injections usually take basal insulin to cover the body's basal insulin needs and additional bolus insulin doses at times when the blood glucose (BG) concentration is high, e.g., around meal times. The challenge in diabetes treatment is that the patient needs to self-reliantly

determine the doses of insulin required to maintain the blood glucose concentration within the normoglycemia range. This means solving an optimization problem several times throughout the day.

To help the patient with this task, blood glucose prediction algorithms as well as many different control algorithms have been proposed [5] [6]. These control algorithms reach from proportional–integral–derivative (PID) control, pole placement over adaptive and run-to-run methods to model predictive control (MPC) [7] [8] [9]. Many of the proposed controllers aim at having a continuous insulin signal injected into the diabetic patient via an insulin pump.

However, in the scope of the European project DIAdvisor$^{\text{TM}}$ [10] [11] aiming at developing a blood glucose prediction and treatment advisory system, the patient should be able to use, e.g., an insulin pen instead of a pump. Whereas continuous insulin administration can be useful for patients using an insulin pump, this is not suitable for patients using for example insulin pens to administer insulin. Instead, insulin dose advices should in such a case be in the form of impulses.

This thesis aimed at developing a control algorithm, that calculates impulse-formed insulin and glucose dose advices. These advices should not be given very frequently, but rather only a few times a day. Here the need for insulin and glucose intakes was determined in case of a meal or if the blood glucose concentration left a safe range. To determine the amounts of insulin and glucose to be taken, two different approaches were proposed. The first approach was to formulate an optimization problem, whose solution gave the amounts of insulin and glucose to be taken. The second approach was to evaluate a cost function for given sets of insulin and glucose intakes. The insulin and glucose doses resulting in the lowest cost were then chosen to be applied to the patient.

The thesis is structured in the following way:

- Chapter 1 gives an introduction, formulates the problem for this thesis and presents the European project DIAdvisor, within which this work was done.

- Chapter 2 gives a background about the *Diabetes Mellitus* disease, how the blood glucose is regulated by the human body and how *Diabetes Mellitus* is treated. Also, an overview of research about automatic control in diabetes is given.

- Chapter 3 presents the nonlinear model used as a virtual patient to

simulate a patient with type 1 diabetes.

- Chapter 4 introduces the mathematical models describing the patient dynamics used in the prediction and control algorithms, since the proposed control algorithms are model-based.

- Chapter 5 describes the optimization-based control algorithm developed in this thesis. The cost function used as well as the formulation of the optimization problem are presented. Furthermore, it is described how this optimization problem was solved and how it was embedded within an algorithm to form a controller.

- Chapter 6 describes the selection-based control algorithm. It is described how different combinations of insulin and glucose intakes were tested with the help of a cost function, in order to choose the insulin and glucose dose combination leading to the smallest cost.

- Chapter 7 describes the simulation environment, the metrics used for controller evaluation and presents the results. Moreover, a bolus calculator serving as a comparative reference for the proposed control algorithm is introduced.

- Chapter 8 discusses the results and Ch. 9 concludes the work.

## 1.1   The DIAdvisor project

The work presented in this thesis was done within the European Project DIAdvisor[TM] [10] [12]. The goal of the project was to develop a mobile short-term blood glucose predictor and treatment advisory system, that helps diabetic patients to manage their therapy, minimize the time spent outside the normal glycemic range and give them an improved quality of life. The negative effects of long-term hyperglycemia, i.e. too high blood glucose values, should be reduced without increasing the occurrence of hypoglycemia, i.e. too low blood glucose values. The objective of the project was to develop a system, which predicts blood glucose levels and gives treatment advice to the patient [10] [12].

The concept of the DIAdvisor[TM] project is shown in Figure 1.1. The DIAdvisor[TM] system incorporates both a blood glucose predictor, predicting the future blood glucose development, and an advisor informing

the patient about corrective actions needed to best reach a blood glucose
target range. It needs inputs provided by the patient, e.g., about meals
and insulin intakes and from sensors such as blood glucose sensors. With
the help of these inputs, the DIAdvisor$^{TM}$ system provides a prediction of
future blood glucose development and based on this calculates advices on
corrective actions in terms of insulin and food intakes. The blood glucose
prediction and advices are given to the patient as an instruction. The pa-
tient then has to administer the doses using, e.g., an insulin pen or pump.
The patient data are also sent to the health care provider.
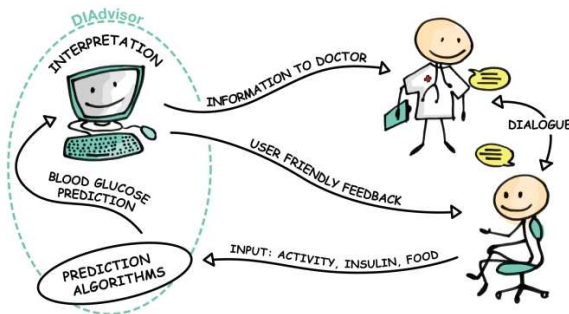


**Figure 1.1**   The concept of the DIAdvisor mobile short-term blood glucose
predictor and treatment advisory system [11].

The DIAdvisor$^{TM}$ system was evaluated in clinical trials at three dif-
ferent sites, collecting data from 50 different patients [12].

Up to date patients decide upon insulin doses either using personal
experience, or using rules of thumbs to calculate the correct insulin dose
based on consumed carbohydrates and measured blood glucose values.
Simple bolus calculators can assist with the calculations. By giving infor-
mation about future blood glucose development and insulin intake recom-
mendations to the patient, the DIAdvisor$^{TM}$ system intends to empower
patients into taking own decisions in their diabetes treatment [12].

## 1.2 Problem Statement: Diabetic Impulse Control

In the sense of the DIAdvisor™ project described in Sec. 1.1, the aim of this thesis was to develop a control algorithm, which gives advice about insulin injections to the patient while still allowing the patient some flexibility during the day. In this context, to keep flexibility means that the dose of insulin is determined when needed, e.g. at mealtime, and does not need to be planned for the whole coming day. To fit the DIAdvisor™ system, advices should not be given in a continuous manner, but instead be in the shape of impulses, and they should be given rather seldom. The control algorithm should determine the doses of insulin and glucose intakes based on blood glucose predictions and measurements. Furthermore, the control algorithm should be based on an individual mathematical patient model describing the patient dynamics. Similar as described in Sec. 1.1, the goal was to minimize time spent outside the normal glycemic range.

## 1.3 Publications

Publications which the thesis is based on:

- M. Cescon, M. Stemmann, and R. Johansson, "Impulsive predictive control of T1DM glycemia: An in-silico study," in *5th Annual Dynamic Systems and Control Conference (ASME 2012), Ft. Lauderdale, FL, USA*, October 17-19 2012

- M. Stemmann and R. Johansson, "Control of type 1 diabetes via risk-minimization for multi dose injection patients," in *5th International Conference on Advanced Technologies and Treatments for Diabetes (ATTD 2012), Barcelona, Spain*, February 8-11 2012

- M. Stemmann and R. Johansson, "Diabetic blood glucose control via optimization over insulin and glucose doses," in *8th IFAC Symposium on Biological and Medical Systems (IFAC BMS 2012), Budapest, Hungary*, August 29-31 2012

Other publications:

- M. Stemmann, F. Stahl, J. Lallemand, E. Renard, and R. Johansson, "Sensor calibration models for a non-invasive blood glucose measurement sensor," in *2010 Annual International Conference of the*

*IEEE Engineering in Medicine and Biology Society (EMBC 2010), Buenos Aires, Argentina*, pp. 4979–4982, August 31 - September 4 2010

# 2

# Background

## 2.1 Blood Glucose Regulation in the Body

Glucose is one of the most important energy sources of the human body and is used as fuel by almost all cells, e.g., muscles, adipose tissue or the cells in the brain. A stable concentration of glucose in the blood is essential. The healthy human body has an in-built, complex feedback system to regulate the concentration of glucose in the blood and make sure it remains in balance. The main regulator of this so called glucose homeostasis is the hormone insulin, which is produced by the $\beta$-cells in the pancreas [17]. It stimulates the uptake of glucose by the cells of insulin-dependent tissue and the storage of glucose in the liver. In addition, there are counter regulatory hormones such as glucagon, epinephrine, cortisol or growth hormone, which work to prevent hypoglycemia, i.e., too low blood glucose concentration [1] [18].

When a patient consumes a meal, the blood glucose concentration increases, which stimulates the pancreas to secrete insulin. Insulin then promotes the utilization of the glucose by insulin-dependent body tissues, such as muscles and adipose tissue, as well as the storage of glucose in the liver and muscles as glycogen, compare to Fig. 2.1. Moreover, it inhibits the liver from producing more glucose and thus brings the blood glucose back to normal. Between meals, when the blood glucose concentration drops, the secretion of insulin from the pancreas is decreased, stimulated by the counter regulatory hormones mentioned above. If the BG con-

centration drops too low, glucose is released into the blood by splitting glycogen from the liver back into glucose [1] [7].
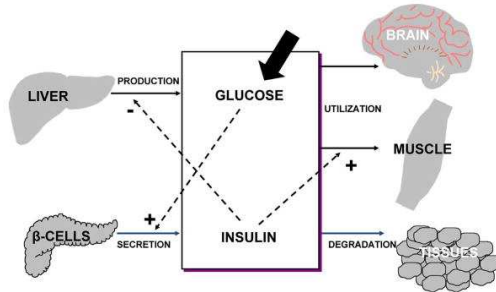


**Figure 2.1**    Scheme of the insulin-glucose regulating system in the body [7]

In a healthy patient, the insulin production is a process that is very closely controlled by the body, and in which the body closely monitors the glucose levels. If the blood glucose levels drop too low nevertheless, there are three mechanisms in the body that should protect from hypoglycemia, i.e., too low blood glucose level [19]. When the blood glucose level drops under the normal level of 80 mg/dL, the release of insulin is decreased and kept at low levels. Moreover, the low glucose level stimulates the glucose production in liver and kidneys in order to increase the blood glucose levels. If the blood glucose level falls further, i.e., below $65 - 70$ mg/dL, the hormone glucagon is released from the alpha cells in the pancreas and also epinephrine is released. Glucagon and epinephrine both stimulate the production of glucose in the liver, while epinephrine also stimulates glucose production in the kidneys. It also induces symptoms that can be felt by the patient like increased heart rate, nervousness or anxiousness. An increased release of cortisol and growth hormone occurs, if the blood glucose level stays low for a prolonged time. If the blood glucose levels fall below 50 mg/dL, cognitive dysfunction, seizures and loss of consciousness may occur, since the delivery of glucose to the brain is insufficient [19].

## 2.2 Diabetes Mellitus

Due to either a deficiency of insulin or the inability of the body to use insulin efficiently, the chronic disease *Diabetes Mellitus*, often only called diabetes, leads to hyperglycemia. There are several kinds of diabetes, each having different pathophysiological mechanisms. The two most common kinds are type 1 and type 2 diabetes [20].

The most common form is type 2 diabetes (T2DM). It mostly appears in adults, but has lately also occurred in children and adolescents [4]. It is caused by a combination of insulin resistance and relative insulin deficiency with increased glucose production in the liver. This means, that the body can usually produce its own insulin, but either the amount is not sufficient, or the body is not responding to its effects, due to a decreased sensitivity of the insulin-dependent tissues to insulin [1] [21] [22]. Some important factors that may promote T2DM are obesity, poor diet, physical inactivity or increasing age. Not all patients require daily insulin injections, instead they are treated with a combination of diet advice, oral medications and physical activity [4]. In later stages of T2DM, deterioration of the pancreas can occur so that daily insulin treatment is necessary.

Type 1 diabetes (T1DM) is characterized by absolute insulin deficiency. Through an autoimmune reaction, the body's own immune system attacks the insulin-producing $\beta$-cells in the pancreas and destroys them. This decreases the ability of the body to produce insulin and eventually leads to hyperglycemia. The first symptoms appear when approx. 80 % of the $\beta$-cells are destroyed. Patients suffering from T1DM need to substitute the missing insulin with externally injected insulin every day to control their blood glucose concentration. To achieve good control, they need to closely monitor their blood glucose concentration and adjust insulin intakes and diet to achieve normal blood glucose levels every day [1] [21] [22].

During long-term high levels of blood glucose concentration, diabetes leads to diseases affecting the heart and blood vessels, eyes, kidneys and nerves. It is one of the main causes of cardiovascular disease, blindness and kidney failure in high-income countries [4].

## 2.3 Insulin

To control hyperglycemia in diabetes, insulin has been used since the 1920s. Pioneering efforts to use insulin in diabetes treatment were made in 1922 [23]. Initially, insulin was extracted from animal pancreatic tissue, but nowadays a recombinant DNA technique employing microorganisms is used to produce insulin [24].

There are different kinds of insulin available with different on-set and duration times. For regular insulin, it takes about 30 to 60 minutes until it starts having an effect. Its peak effect is reached after $2 - 3$ hours and the total duration is 8 to 10 hours [24]. It is a short acting insulin that is used to cover meal-time glucose excursions. Through modification and combination with additives at the molecular level, the insulin can be modified to be absorbed more quickly. Such modified insulin analogs reach the maximum peak in less time and have a higher maximum insulin concentration [24].

Regular insulin can also be modified to prolong its pharmacokinetic profile. This modification is called long-acting insulin and is used to replace the body's long acting insulin requirements. One such long-acting insulin is for example NPH (neutral protamine Hagedorn), with an onset action after 2 to 4 hours, a peak action after 4 to 10 hours and a duration of 10 to 16 hours [24]. There are also other long-acting insulins available, which have different maximum peak or half-life. Glargine for example has a reduced peaking effect, an on-set of 1-2 hours and a duration of 20-30 hours [25].

## 2.4 Diabetes Treatment

For both T1DM and T2DM, lifestyle treatment consisting of a healthy diet and regular physical exercise is important. Because of the absolute insulin deficiency in patients with T1DM, these patients need to be treated with externally administered insulin intakes [24].

The conventional therapy consists of one or two injections of intermediate and rapid-acting insulin per day, and includes self-monitoring of urine or blood glucose as well as education about diet and exercise. This therapy approach does not include daily adjustments of insulin doses [26], which means that a strict daily schedule of meal times with little flexibility

is required.

A more intensive approach [26] consists of long-acting insulin analogs, that are administered one to two times per day, to cover the body's basal insulin requirements and rapid-acting insulin analogs to cover meal-times. The amount of rapid-acting insulin is determined according to the amount of carbohydrates in a meal, considering the measured blood glucose concentration at mealtime. The total amount of insulin injections needed each day are larger than with the conventional approach, but the intensive approach replicates more closely the body's insulin secretion. It also allows for a greater flexibility concerning mealtimes [24].

A major risk for patients treated with any kind of insulin therapy is hypoglycemia, which can be life threatening [18]. While the intensive insulin treatment is associated with a decrease in micro vascular complications and decreased risk of kidney failure, it increases the risk for hypoglycemia [26]. The drop of blood glucose can be induced not only by too large insulin administration, but also by increased activity or decreased appetite among others. To prevent hypoglycemia, patients are presented with the task to match the rate of insulin into the bloodstream with the rate of glucose entering the bloodstream, only by subcutaneous insulin injections. Usually patients estimate the amount of glucose in the meal and use a carbohydrate-to-insulin ratio to determine the amount of insulin that is needed to cover the meal. Furthermore, patients calculate the amount of insulin necessary to lower the blood glucose concentration using an insulin sensitivity factor. These ratios and factors are determined with the help of the health care provider. Factors like stress and physical activity can alter the amount of insulin needed. This means that these patients have to solve an optimization problem every day [19].

## 2.5  Automatic Control for Diabetes

Many efforts have been made to develop control algorithms that help with the therapy for diabetic patients. The first closed-loop algorithms were established in the '60s and '70s and used intravenous glucose measurements and insulin infusion. In [27] and [28] for example, a hyperbolic tangent function relating BG concentration and rate of change to insulin infusion rate is used as a control law. The first product commercially available was the Biostator [29] [30].

In [31], the feasibility of using subcutaneous glucose measurements and insulin infusions for closed-loop control of diabetes was shown using PID control, which became a widely researched algorithm for control of diabetes [32] [33] [34].

More recently, the most commonly used algorithm for closed-loop control in diabetes is the model predictive control (MPC) algorithm [7] [8] [9] [30]. As the name suggests, it includes a model of the patient metabolic system. Since predictions of the future development of the blood glucose concentration are possible, the effect of insulin on the future blood glucose concentration can be determined. Furthermore, constraints can be included to take into account limitations on, e.g., insulin delivery and the permitted blood glucose concentration of the patient.

MPC has in earlier years been developed for intravenous insulin infusions and glucose measurements, e.g., in [35], [36], where an MPC with constraints on the insulin infusion rate was used. In [36], glucose infusion was added as an additional controlled variable. Furthermore, an asymmetric cost function was used to take into consideration that hypoglycemia is much more dangerous than hyperglycemia.

Later, MPC was mainly used with subcutaneous glucose measurements and insulin infusions. Using an unconstrained MPC controller gave performance improvements over PID control [37] in in-silico trials. To include a prediction of the amount of insulin available in the blood over time after an intake of insulin, insulin on board (IOB) was incorporated into the MPC controller [38]. An approach to combine the advantages of MPC control with conventional therapy to cover disturbances like meals was presented in [39]. The conventional therapy was used as a feed-forward compensation, while the MPC controller provided feedback control to cover, e.g., meal uncertainties. A way to adjust the controller parameters on a day to day basis was done in [40] by adapting the MPC controller parameters with a run-to-run strategy.

An advisory algorithm based on fuzzy control, which determines the amounts of insulin to be injected by patients using multiple insulin doses per day instead of a pump, was developed in [41]. Using expert knowledge about diabetes treatment, the amounts of insulin to be injected were determined on a day to day basis. Another algorithm aimed at determining insulin doses for patients using multiple daily insulin injections based on run-to-run control was developed in [42], which assumed a prescribed diet regime for the patient.

In [43], basal insulin infusion rate and bolus insulin intakes were calculated using inversion via interval analysis, which determined a set of bolus intakes and basal infusion rates guaranteeing a good postprandial blood glucose response.

An approach to fit the MPC control scheme to optimize therapy for patients using multiple insulin doses per day was presented in [44]. The control signal determined by the MPC controller was approximated by single control outputs at single time points through summation of the MPC controller's output signal. To take into account different patient dynamics for different blood glucose concentrations, gain scheduling was used. In an in-silico study it was found that approximating the insulin signal determined by the MPC by single insulin injections did not reduce the performance significantly.

# 3

# The Virtual Patient

In order to test the developed control algorithm in closed-loop, a type 1 diabetes Virtual Patient [45] was implemented. The Virtual Patient is a complex, nonlinear model simulating the glucose-insulin system in the body. Originally developed for meal simulation, it describes the physiological events happening in the glucose-insulin system after a meal intake by using compartment modeling [45]. The parameters were identified using measurements of various fluxes and plasma concentrations of insulin and glucose [46].

This nonlinear model was implemented in Matlab and Simulink [47], serving as a simulated patient with type 1 diabetes to allow control algorithms to be tested in closed-loop. Three different sets of parameters were provided though the DIAdvisor$^{\text{TM}}$ project, so that three different patients could be simulated.

Figure 3.1 shows how the whole system is divided into several parts, connected through fluxes of insulin and glucose.

***Glucose System*** The glucose system consists of two compartments. The first compartment describes the insulin-independent glucose utilization in, e.g., the brain, kidneys and red blood cells. The second compartment describes insulin-dependent glucose utilization in, e.g., muscle and adipose tissue. Equation (3.1) shows the model describing the glucose
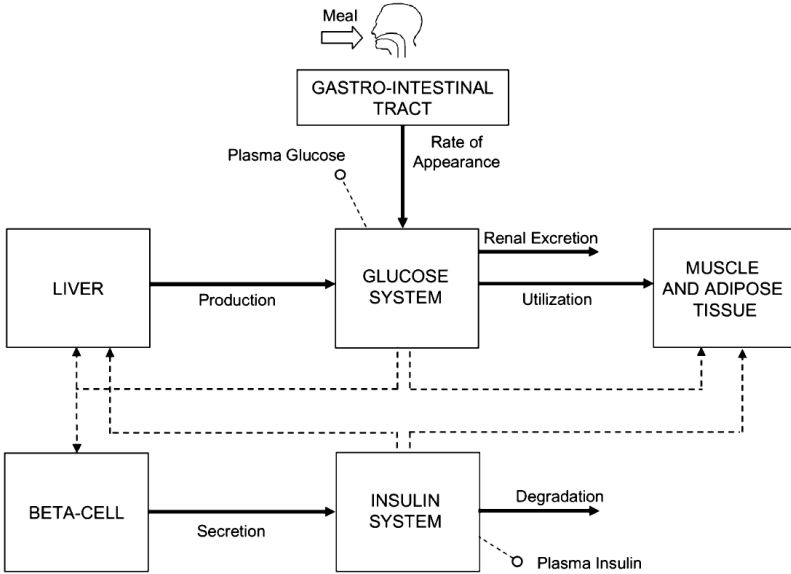
**Figure 3.1** Scheme of the glucose-insulin system. The continuous lines denote fluxes of insulin or glucose, the dashed lines denote insulin or glucose signals controlling the sub-parts of the virtual patient. [46]

kinetics in the glucose system [46].

$$\dot{G}_p(t) = \max\{0, \dot{G}_{\text{EGP}}(t)\} + R_a(t) + U_{ii}(t) + E(t) \qquad (3.1)$$
$$+ k_1 \cdot G_p(t) + k_2 \cdot G_t(t)$$
$$\dot{G}_t(t) = -U_{id} + k_1 \cdot G_p(t) - k_2 \cdot G_t(t)$$
$$G(t) = \frac{G_p(t)}{V_g}$$

The glucose masses in plasma and rapidly equilibrating tissues, and in slowly equilibrating tissues are denoted by $G_p(t)$ and $G_t(t)$ [mg/kg], respectively. The plasma glucose concentration is denoted by $G(t)$ [mg/dL], the endogenous glucose production by $\dot{G}_{\text{EGP}}(t)$ [mg/kg/min], the glucose rate of appearance in plasma by $R_a(t)$ [mg/kg/min] and the renal excretion by $E$ [mg/kg/min]. The insulin-independent and insulin-dependent

glucose utilization are denoted by $U_{ii}$ and $U_{id}$ [mg/kg/min], respectively. The distribution volume of glucose is $V_g$ [dL/kg] and $k_1$ and $k_2$ are parameters [min$^{-1}$] [46].

*Renal Excretion* of insulin occurs when the glucose in plasma exceeds the threshold $k_{e2}$. This is modeled as follows:

$$E(t) = \begin{cases} k_{e1}[G_p(t) - k_{e2}] & \text{if } G_p(t) > k_{e2} \\ 0 & \text{if } G_p(t) \leq k_{e2} \end{cases} \tag{3.2}$$

**Insulin System** The Insulin System consists of two compartments as well. The first compartment represents the liver and the second compartment the plasma. Degradation of insulin happens in both compartments. Eq. (3.3) shows the insulin kinetics.

$$\dot{I}_l(t) = -(m_1 + m_3) \cdot I_l(t) + m_2 \cdot I_p(t) \tag{3.3}$$
$$\dot{I}_p(t) = -(m_2 + m_4) \cdot I_p(t) + m_1 \cdot I_l(t) + S(t)$$
$$I(t) = \frac{I_p(t)}{V_i}$$

The insulin masses in plasma and liver are denoted by $I_p$ and $I_l$ [pmol/kg], respectively, and the plasma insulin concentration by $I$ [pmol/l]. The insulin secretion is denoted by $S$ [pmol/kg/min], the distribution volume of insulin by $V_i$ [l/kg] and $m_1$, $m_2$, $m_3$ and $m_4$ are rate parameters [min$^{-1}$].

**Gastro-Intestinal Tract** It provides the glucose rate of appearance for the glucose system after a meal intake, describing the transit of glucose through the stomach and the upper small intestine with three compartments [48]. The first two compartments represent the solid and the liquid phase of the stomach and the third one represents the intestine. The model equations for the glucose absorption are shown in Ep. (3.4)

$$Q_{sto} = Q_{sto1} + Q_{sto2} \tag{3.4}$$
$$\dot{Q}_{sto1}(t) = -k_{gri}Q_{sto1}(t) + d(t)$$
$$\dot{Q}_{sto2}(t) = k_{gri}Q_{sto1}(t) - k_{gut}(t, Q_{sto})Q_{sto2}$$
$$\dot{Q}_{gut}(t) = k_{gut}(t, Q_{sto})Q_{sto2} - k_{abs}Q_{gut}(t)$$
$$R_a(t) = \frac{f k_{abs}}{W_{\text{body}}}Q_{gut}$$

Here $Q_{sto}$ [mg] is the amount of glucose in the stomach, where $Q_{sto1}$ [mg] represents the solid phase and $Q_{sto2}$ [mg] the liquid phase. The glucose mass in the intestine is denoted by $Q_{gut}$ [mg], $k_{gri}$ [min$^{-1}$] denotes the rate of grinding and $k_{abs}$ [min$^{-1}$] the rate constant of intestinal absorption. The fraction of intestinal absorption that appears in the plasma is $f$, and $d$ [mg/min] is the rate of ingested glucose. The body weight is denoted by $W_{\text{body}}$ [kg] and the rate of appearance of glucose in the plasma by $R_a$ [mg/kg/min]. The rate constant of gastric emptying $k_{gut}(t, Q_{sto})$ [min$^{-1}$] is a nonlinear function of $Q_{sto}$:

$$k_{gut}(t, Q_{sto}) = k_{min} + \frac{k_{max} - k_{min}}{2} \cdot \{\tanh[\alpha(Q_{sto} - b\bar{D}(t))] \qquad (3.5)$$
$$- \tanh[\beta(Q_{sto} - a\bar{D}(t))] + 2\}$$

with

$$\alpha = \frac{5}{2\bar{D}(t)(1 - b_v)}$$
$$\beta = \frac{5}{2\bar{D}(t)a_v}$$
$$\bar{D}(t) = Q_{sto} + \int_{\bar{t}_s}^{\bar{t}_f} d(\tau)d\tau$$

where $\bar{t}_s$ and $\bar{t}_f$ are the initial and final time of the last glucose ingestion and $a_v$, $b_v$, $k_{min}$ and $k_{max}$ are model parameters. For details see [48]. Figure (3.2) shows the glucose rate of appearance $R_a(t)$ as a response to 10 g carbohydrate intake for the three different virtual patients.

**Endogenous Glucose Production** The endogenous glucose production by the liver is controlled by a glucose and an insulin signal. The model equations are shown in Eq. (3.6).

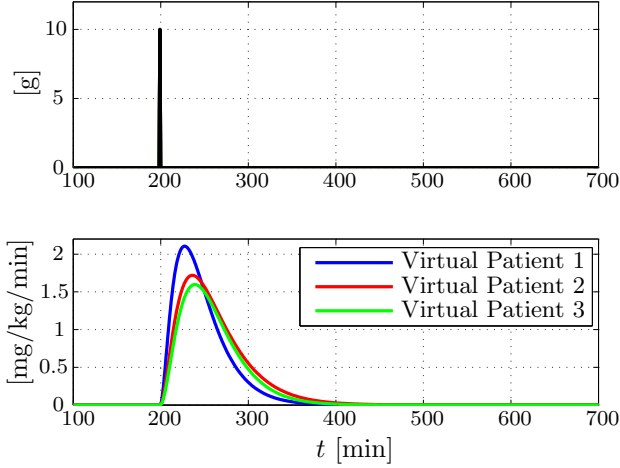$$\dot{G}_{\text{EGP}}(t) = k_{p1} - k_{p2}G_p(t) - k_{p3}I_d(t) \qquad (3.6)$$

The delayed insulin signal $I_d$ [pmol/l] is given through Eq. (3.7).

$$\dot{I}_1(t) = -k_{ins}(I_1(t) - I(t)) \qquad (3.7)$$
$$\dot{I}_d(t) = -k_{ins}(I_d(t) - I_1(t))$$

Here $I$ [pmol/l] is the plasma insulin concentration, $k_{p1}$ [mg/kg/min] is the extrapolated $\dot{G}_{\text{EGP}}(t)$ at zero glucose, $k_{p2}$ [min$^{-1}$] is the liver glucose

**Figure 3.2** Glucose rate of appearance $R_a(t)$ (lower panel) as a response to 10 g glucose intake (upper panel).

effectiveness, $k_{p3}$ [mg/kg/min/(pmol/l)] is a parameter that influences the amplitude of insulin action on the liver and $k_{ins}$ [min$^{-1}$] is a parameter describing the delay between the insulin signal and insulin action.

*Muscle and adipose tissue* The glucose is utilized by the muscle and adipose tissue, which is as well controlled by insulin and glucose signals. The model equations are shown in Eq. (3.8).

$$U_{id}(t) = \frac{V_m(t)G_t(t)}{K_m + G_t(t)} \tag{3.8}$$
$$V_m(t) = V_{m0} + V_{mx}X(t)$$
$$\dot{X}(t) = -p_{2U}X(t) + p_{2U}[I(t) - I_b]$$

Here $X(t)$ [pmol/l] denotes the remote insulin, $I_b$ is the basal insulin, $I$ denotes the plasma insulin, $p_{2U}$ is a rate constant of insulin action on peripheral glucose utilization and $K_m$, $V_{m0}$ and $V_{mx}$ are model parameters, see [48] for details.

*Subcutaneous Insulin Infusion* The insulin secretion by the $\beta$-*cell* is controlled by a glucose signal. However, since the virtual patient is to
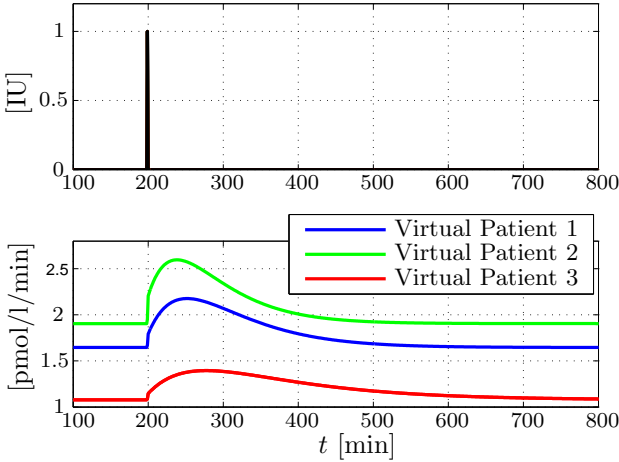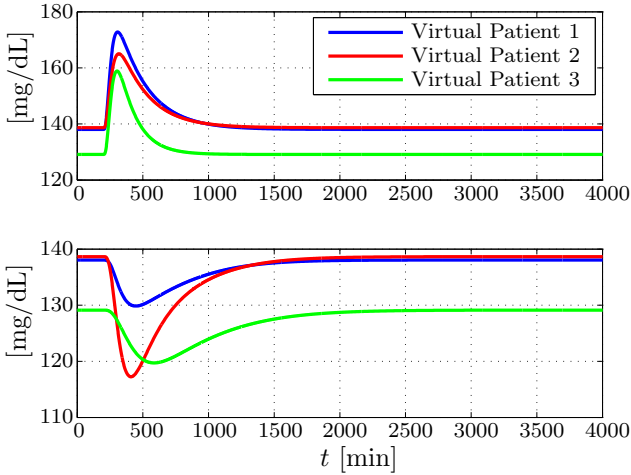
**Figure 3.3**    Insulin rate of appearance $R_i(t)$ (lower panel) as a response to 1 unit insulin intake (upper panel).

be used to simulate a patient with type 1 diabetes, the $\beta$-cell secretion block is substituted by a module describing subcutaneous insulin infusion. This module introduces a higher endogenous glucose production as well. All other parameters are kept unchanged, assuming the patient is in good control [45]. The model equations for the subcutaneous insulin kinetics are shown in Eq. (3.9).

$$\dot{I}_{sc1}(t) = R_{Inf}(t) - (k_d + k_{a1})I_{sc1}(t) \tag{3.9}$$
$$\dot{I}_{sc2} = k_d I_{sc1}(t) - k_{a2}I_{sc2}(t)$$
$$R_i(t) = k_{a1}I_{sc1}(t) + k_{a2}I_{sc2}(t)$$

Here $I_{sc1}$ is the amount of nonmonomeric insulin in the subcutaneous space, $I_{sc2}$ is the amount of monomeric insulin in the subcutaneous space, $R_{Inf}(t)$ [pmol/kg/min] is the infusion rate of exogenous insulin, $k_d$ [min$^{-1}$] is the rate constant of insulin dissociation and $k_{a1}$ [min$^{-1}$] and $k_{a2}$ [min$^{-1}$] are rate constants connected to nonmonomeric and monomeric insulin absorption. The rate of appearance of insulin in plasma is denoted by

**Figure 3.4** blood glucose concentration of the three virtual patients as a response to 10 g of glucose intake (upper panel) and 1 unit of insulin (lower panel).

$R_i(t)$. Figure 3.3 shows the insulin rate of appearance $R_i(t)$ [pmol/kg/min] as an answer to an intake of 1 unit insulin for the three virtual patients. Note that $R_i(t)$ does not start at zero, since the effect of the bolus insulin of 1 unit given to the virtual patient on the insulin rate of appearance is added to a basal level of insulin.

***Insulin Rate of Appearance*** Since the virtual patient simulates a patient with type 1 diabetes, in Eq. (3.3) the insulin rate of appearance $R_i$ in the blood after subcutaneous insulin infusion is used instead of the insulin secretion $S$, so that:

$$S(t) = R_i(t) = k_{a1}I_{sc1} + k_{a2}I_{sc2}(t) \qquad (3.10)$$

Figure 3.4 shows the blood glucose concentration of the three virtual patients as a response to 10 g of carbohydrates (upper panel) and 1 unit of insulin (lower panel). Note that throughout this thesis, the basal rate needed to stabilize the virtual patient without insulin or glucose intakes is provided to the virtual patients.

The model presented in this chapter will be used as a virtual patient to simulate patients with type 1 diabetes. Using this virtual patient allows for closed-loop testing of proposed control algorithms.

# 4

# Patient Models and Predictions

The control algorithms proposed in this thesis to calculate the doses of insulin and glucose were based on a mathematical model of the patient dynamics. Moreover, they used predictions of the blood glucose concentration to take decisions about insulin and glucose intakes. Hence, models of the glucose-insulin dynamics of the diabetic patient were needed.

Two different model structures were used to describe the dynamics of the diabetic patient to be controlled. While the model in the previous chapter served as a simulator of virtual patients, the models presented here were used in the control and prediction algorithms. These models are lower in complexity than the nonlinear model used as a virtual patient. A linear state-space model was used in a prediction algorithm to predict future blood glucose concentration. A hybrid model structure, describing the same dynamics, was used within an opimization-based control algorithm to determine the amounts of insulin and glucose to be applied to the virtual patient. The second, selection-based, control algorithm presented in this thesis used the state-space model as well to describe the patient dynamics.

In this chapter, these two models and the prediction algorithm are presented.

## 4.1 State-Space Model

The linear state-space model used in the prediction algorithm and in one of the control algorithms to describe the insulin-glucose dynamics of a diabetis patient is shown in Eq. (4.1).

$$x_{k+1} = Ax_k + Bu_k + Ke_k \qquad (4.1)$$
$$y_{M,k} = Cx_k + e_k$$

Here, the input $u_k$ is a vector including the insulin rate of appearance $R_i(t)$ and glucose rate of appearance $R_a(t)$ as in Eq. (3.10) and Eq. (3.4), respectively. The output $y_{M,k}$ is the blood glucose concentration in [mg/dL].

Since a discrete time model was to be estimated, the rates of appearance and the blood glucose concentration at the output of the virtual patient were sampled with 1 minute sampling time. For model estimation, the function `n4sid.m` from the Matlab System Identification Toolbox [49] was used, following guidelines in [50].

The estimation data consisted of 24 glucose intakes $a_g$ [g] distributed over 9 days and 24 insulin intakes $a_i$ [IU] for all three patients, which were placed in between the glucose intakes. The data for patient 2 is shown in Fig. 4.1. The sizes and times of the intakes were not chosen in a physiologically correct manner, but in order to get a good fit between the output of the estimated model and the output of the virtual patient. A discussion about identifying patient models using data measured from real patients can be found in, e.g., [50] and [51].

For validation data, a data set of 3 days was taken, with meals three time per day and reasonable amounts of glucose in the meals. The insulin dose was given with the meal and its size was chosen in order to cover the carbohydrate amount of the meal, according to, e.g., [52].

A state-space model was estimated using `n4sid` for model orders between 1 and 12 for the three virtual patients. The model with the model order leading to the best FIT value for a 300 steps ahead prediction for both estimation and validation data was chosen. The FIT value FIT $[\%] = (1 - (||y_{BG} - y_M||)/(||y_{BG} - \bar{y}_{BG}||)) \cdot 100$, where $y_{BG}$ is the blood glucose concentration at the output of the virtual patient, $\bar{y}_{BG}$ its mean value and $y_M$ the output of the estimated model, represents the percentage of the output variation that is explained by the estimated model [49] and was
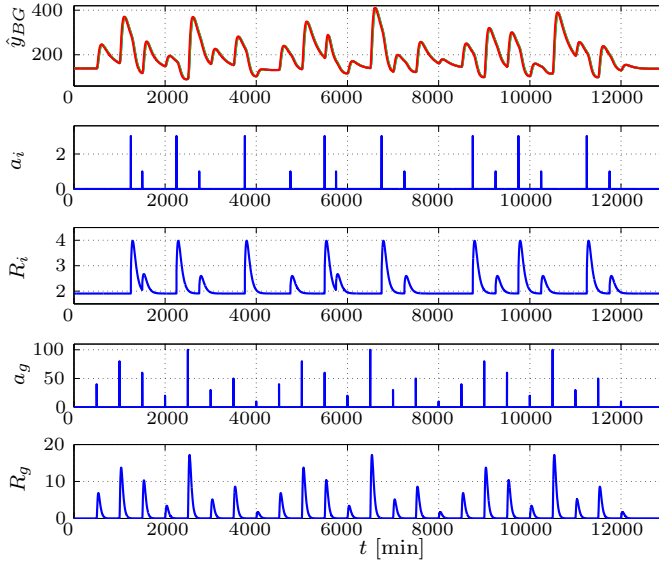
**Figure 4.1**   The data used for estimating the state-space model for patient 2.

calculated for the 300 step ahead prediction using the Matlab function `compare.m`. For the validation data, a FIT of 86%, 88% and 87% could be reached for virtual patients 1, 2 and 3, respectively.

## 4.2  Predictions

Since the control algorithms used predictions of the blood glucose concentration to determine the amounts of glucose and insulin to be applied to the patient, a prediction algorithm was needed. This prediction algorithm used the state-space model in Eq. (4.1) to estimate the blood glucose concentration at the output of the virtual patient for a future horizon $H_p$.

With the state-space model in Eq. (4.1), the blood glucose concentration $p$ time steps ahead can be determined, where $k$ is the actual time

step, see Eq. 4.2.

$$\hat{y}_{k+p} = CA^p x_k + \sum_{m=0}^{p-1} CA^{p-1-m} Bu_{k+m} \qquad (4.2)$$

Collecting the predictions for $p = 1...H_p$ in one vector $\hat{\mathcal{Y}}_{H_p}$ results in Eq. (4.3), representing all blood glucose predictions for the prediction horizon $H_p$.

$$\hat{\mathcal{Y}}_{H_p} = \mathcal{S}_x x_k + \mathcal{S}_u \mathcal{U}_{H_p} \qquad (4.3)$$

with

$$\hat{\mathcal{Y}}_{H_p} = (\, \hat{y}_{k+1} \quad ... \quad \hat{y}_{k+H_p} \,)^T$$
$$\mathcal{U}_{H_p} = (\, u_k \quad ... \quad u_{k+H_p} \,)^T$$

$$\mathcal{S}_x = (\, CA \quad CA^2 \quad ... \quad CA^{H_p} \,)^T$$

$$\mathcal{S}_u = \begin{pmatrix} CB & D & 0 & 0 & ... & 0 \\ CAB & CB & D & 0 & ... & 0 \\ \vdots & \vdots & \ddots & \ddots & \ddots & \vdots \\ CA^{H_p-1}B & CA^{H_p-2}B & ... & CB & D & 0 \\ CA^{H_p}B & CA^{H_p-1}B & ... & CAB & CB & D \end{pmatrix}$$

where here $D = 0$.

The states $x_k$ of the patient model were estimated using a Kalman filter [53]. The inputs $u_i$ for $i = k...k + p - 1$ were the glucose and insulin rate of appearance calculated for the future horizon $H_p$. The rates of appearance were determined from the insulin and glucose intakes using Eq. (3.4) and Eq, (3.9), respectively.

## 4.3 Controller Model

The optimization-based control algorithm proposed in this thesis nedded a model having single insulin and glucose intakes as inputs, not their

rates of appearance, and the change in blood glucose concentration as a response to those inputs over time as an output. A model in this form can be found in [54] [55], which was used here.

For use in a discrete optimization problem, this model was discretized with sampling time $h$, here $h = 1$ min. The sampling instant is denoted by $k$.

The model takes the doses and times of glucose or insulin intakes as inputs and has the change of blood glucose concentration over time as an output. Equation (4.4) shows this model for insulin and glucose intakes, where $y_{h,g}(k, k_g, a_g)$ is the change in blood glucose concentration as response to a glucose intake of size $a_g$ [g] at time $t_g = h \cdot k_g$ [min] and $y_{h,i}(k, k_i, a_i)$ the change in blood glucose concentration for an insulin intake with the size $a_i$ [IU] at time $t_i = h \cdot k_i$ [min]. The model is linear in the intake doses $a_i$ and $a_g$.

$$
\begin{aligned}
y_{h,g}(k; k_g, a_g) &= \begin{cases} n_1 e^{-n_2 h(k-k_g)} h^{n_3} (k - k_g)^{n_3} a_g & \text{if } k \geq k_g \\ 0 & \text{else} \end{cases} \quad (4.4) \\
y_{h,i}(k; k_i, a_i) &= \begin{cases} n_4 e^{-n_5 h(k-k_i)} h^{n_6} (k - k_i)^{n_6} a_i & \text{if } k \geq k_i \\ 0 & \text{else} \end{cases}
\end{aligned}
$$

The parameters $n_1$ to $n_6$ were estimated individually for the patient to be controlled. This was done using nonlinear constrained optimization [56], solving the optimization problem (4.5). The blood glucose concentration at the output of the virtual patient is denoted by. An initial offset $c_{\text{offset},BG}$ in the blood glucose data $y_{BG}$ was subtracted from $y_{BG}$. The parameters $n_1$ and $n_4$ were constrained to ensure a physiologically correct gain of the model considered.

$$
\begin{aligned}
\min_{n_1 \dots n_6} &\sum_{k=0}^{N} |y_{h,g}(k; k_g, a_g) + y_{h,i}(k; k_i, a_i) - (y_{BG}(k) - c_{\text{offset},BG})|^2 \quad (4.5) \\
&n_1 > 0 \\
&n_4 < 0
\end{aligned}
$$
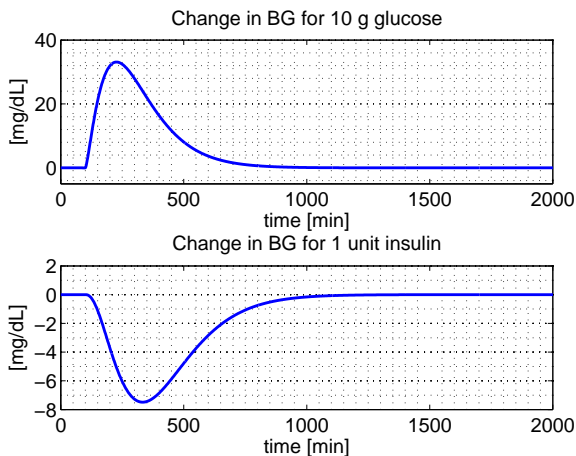
**Figure 4.2**   Output of the nonlinear model for patient 2. Upper panel: Change of BG as response to 10 g of Glucose intake at time $t_g = 100$. Lower panel: Change of BG as response to 1 unit of insulin intake at time $t_i = 100$.

Figure 4.2 shows $y_{h,g}(k, k_g, a_g)$ and $y_{h,i}(k, k_i, a_i)$ with $a_g = 10$ g and $a_i = 1$ unit at times $k_g = k_i = 100$ as inputs for a sample patient. To form the total change of blood glucose concentration from an initial value when both insulin and glucose are taken at different times, those two functions were added.

Note that both $y_{h,g}(k, k_g, a_g)$ and $y_{h,i}(k, k_i, a_i)$ start at zero, since they descibe the deviation of the blood glucose concentration caused by intakes of insulin or glucose.

The model presented here was used in the optimization-based control algorithm to describe the effects of intakes of insulin and glucose on the blood glucose concentration. Based on this and predictions of future blood glucose concentration, the optimization-based control algorithm calculated doses of insulin and glucose.

# 5

# Diabetic Glycemia Control via Optimization

The proposed control algorithm determined the amounts of insulin and glucose a patient with type 1 diabetes should take in order to bring the blood glucose concentration back to normoglycemia through solving an optimization problem. This optimization problem was solved at distinct points in time, e.g., when a meal occurs or when the blood glucose concentration left the normal range of $70 - 180$ [mg/dL]. Hence, the insulin and glucose control signals were pulse shaped.

While insulin treatment is important in most of the every day situations, additional glucose intakes can be important to prevent hyperglycemia under special conditions like exercise or stress [1]. Therefore, apart from insulin dose advice, also glucose dose advices were determined by the control algorithm proposed in this chapter.

The structure of the control loop is shown in Fig. 5.1. A *virtual patient* as described in Sec. 4.3 was used to simulate the diabetic patient to be controlled. A *prediction* algorithm (see Sec. 4.2) determined the blood glucose concentration in a future horizon using information about the blood glucose concentration at the output of the virtual patient and the insulin and glucose applied to the virtual patient. The *controller* used the blood glucose predictions and the blood glucose concentration at the output of the virtual patient in an optimization algorithm to determine the amount of insulin and glucose the patient should take. The optimization problem was solved at specific points in time. When a meal occured or when the blood glucose concentration was predicted to leave the normal
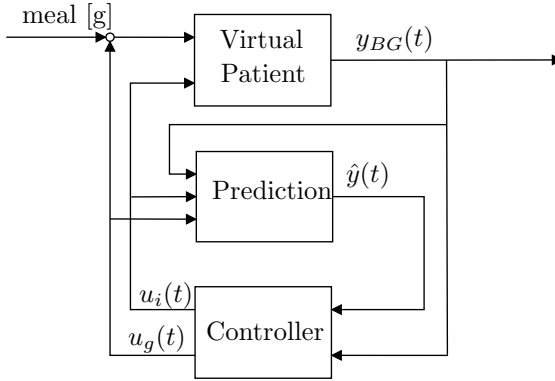
**Figure 5.1** The structure of the control algorithm.

range of $70 - 180$ [mg/dL], the optimization was called to determine the dose of insulin and glucose that should be administered to the virtual patient.

This chapter is organized as follows. First, the cost function used by the optimization problem is introduced. Next, the optimization problem is formulated and last, the control algorithm invoking the optimization problem is described.

## 5.1 The Asymmetric Cost Function

The cost function used in the optimization problem had an asymmetric shape over the blood glucose concentration. The reason for this was that low blood glucose values were associated with much worse complications than high blood glucose values. Through the asymmetric shape, the cost function in Eq. (5.1) [57] used here took this circumstance into account.

$$J = \sum_{k=k_0}^{H_p} L(k) \tag{5.1}$$

$$L(y(k)) = a \cdot y(k) + b + c \cdot \max\{(d - y(k))^3, 0\}$$
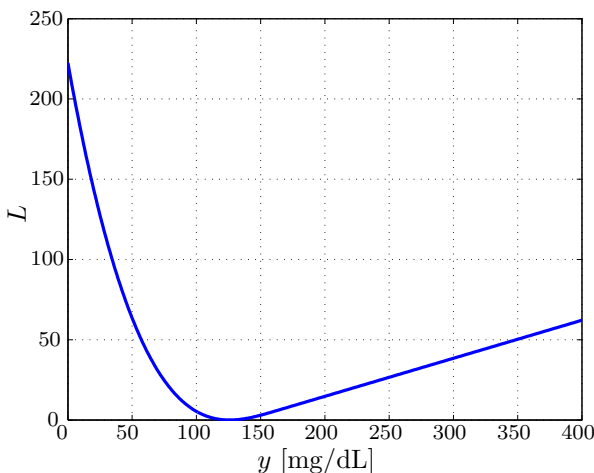
**Figure 5.2**   The asymmetric cost function in Eq. (5.1).

The advantage of an asymmetric over a quadratic cost function for control was already addressed in [58] and [59] for example.

The BG concentration is denoted by $y(k)$. The time at which the optimization algorithm is called is denoted by $k_0$ and the prediction horizon over which the blood glucose concentration $y(k)$ is predicted is $H_p = 120$ [min] (compare to Sec. 4.2). The parameters $a$, $b$, $c$ and $d$ have been adjusted to have a the minimum of the asymmetric cost $L(y(k))$ at 126 [mg/dL], so that $a = 0.237$, $b = -32.66$, $c = 6 \cdot 10^{-5}$ and $d = 162$. Figure 5.2 shows $L$ over the blood glucose concentration $y$. One of the advantages of the cost function (5.1) over, e.g., the asymmetric cost presented in [60] is that it is convex. The convexity is shown in Appendix A.

For the optimization problem convexity means that the optimal solution to the problem is guaranteed to be found [61].

A technical advantage of the cost function (5.1) is that it handles negative blood glucose values [57]. This is valuable because large insulin intakes, which the prediction algorithm expects to lead to negative blood glucose values, need to be taken into account in order to be avoided.

45

## 5.2 The Optimization Problem

In order to determine the amounts of insulin and glucose to be taken by the diabetic patient, an optimization problem was solved. The solution to this problem was calculated if a meal occured, if the blood glucose concentration was predicted to fall below 80 [mg/dL] or if it rose over 180 [mg/dL], see also Sec. 5.3. The optimization used the predicted blood glucose values $\hat{y}$ from Eq. (4.2) and added the effect of insulin and glucose intakes on the blood glucose concentration according to Eq. (4.4). Together, they form the expected future blood glucose concentration as shown in Eq. (5.2):

$$y(k; a_g, a_i) = y_{h,g}(k; k_g, a_g) + y_{h,i}(k; k_i, a_i) + \hat{y}(k) \qquad (5.2)$$

The effect that intakes of insulin and glucose have on the blood glucose concentration is denoted by $y_{h,i}(k; k_i, a_i)$ and $y_{h,g}(k; k_g, a_g)$, respectively. The size of the insulin intake $a_i$ and the size of the glucose intake $a_g$ are the optimization variables to be determined by the optimization problem. The times of insulin and glucose intake $k_i$ and $k_g$ were set before the optimization problem was solved. Hence, in Eq. (5.2), $y(k; a_g, a_i)$ depends linearly on the dose sizes and not on the intake times.

The optimization problem to be solved is shown in Eq. (5.3).

$$\underset{a_i, a_g}{\text{minimize}} \sum_{k=1}^{H_p} \left[ a \cdot (y_{h,g}(k; k_g, a_g) + y_{h,i}(k; k_i, a_i) + \hat{y}(k)) + b \right. \qquad (5.3)$$
$$\left. + c \cdot \max\{(d - (y_{h,g}(k; k_g, a_g) + y_{h,i}(k; k_i, a_i) + \hat{y}(k)))^3, 0\} \right]$$
$$+ c_3 \cdot |a_i| + c_4 \cdot |a_g|$$

subject to
$$0 < a_i < c_{\text{lim,i}}$$
$$0 < a_g < c_{\text{lim,g}}$$

It used the cost function (5.1), where the blood glucose concentration $y(k)$ was substituted by Eq. (5.2). This gives a cost function, which depends on the size of the insulin dose $a_i$ [IU] and the size of the glucose dose $a_g$ [g]. Since Eq. (5.2) is affine in $a_i$ and $a_g$ and the cost function (5.1) is convex,

the composition is convex as well [61]. Linear constraints were added to the optimization problem, which constrained the amount of insulin and glucose determined by the optimization. The convex cost function and the linear constraints on the optimization variables give a convex optimization problem.

## Solving the Optimization Problem

To solve the optimization problem (5.3), the Optimization Toolbox from Matlab [56] was used. This toolbox offers algorithms to solve constrained and unconstrained optimization problems. Among others, functions for linear, quadratic and nonlinear optimization are available.

The optimization problem (5.3) had a smooth and nonlinear cost function with more than one optimization variable. The constraints were bounds on the optimization variables. Therefore, the function `fmincon` was used to solve (5.3). This function solves constrained optimization problems in the form shown in Eq. (5.4).

$$\underset{z}{\text{minimize}}\ f(z) \tag{5.4}$$
$$\text{subject to}$$
$$G_i(z) = 0, i = 1, ..., m_e$$
$$G_i(z) \leq 0, i = m_e + 1, ..., m$$

The function $f(z)$ is the cost function to be minimized over the optimization variables in the vector $z$, where $f(z)$ can be nonlinear. The constraints $G_i(z)$ represents the constraints on the optimization problem. There are $m_e$ equality constraints and $m - m_e$ inequality constraints, which can be nonlinear as well. Comparing this to the optimization problem (5.3), the cost function $f(z)$ was the nonlinear function $J$ in Eq. (5.1), where $y(k)$ was substituted by $y(k; a_i, a_g)$ in Eq. (5.2). The optimization variables were the doses of insulin and glucose, i.e., $z = [a_g\ a_i]$. There were no equality constraints, but linear inequalities to limit the allowed doses for insulin and glucose.

The active-set algorithm was used here within `fmincon` to solve the optimization problem. The active-set algorithm does not need a gradient to be provided and it can take large steps, to improve simulation speed

[56]. The optimization variables, i.e. the amount of insulin and glucose, were constrained to be positive.

## 5.3 The Control Algorithm

The control algorithm took predictions $\hat{y}$ of the blood glucose concentration during a future horizon, as produced by the predictor (see Sec. 4.2), and the actual measured blood glucose concentration as inputs, and gave out values for the amount of insulin and glucose to be taken. Meals taken by the virtual patient were, if not stated otherwise, assumed to be unknown disturbances.

The amount of glucose and insulin to be taken was determined through the optimization problem (5.3). This was solved in the following cases:

**1)** A meal occured,

**2)** The blood glucose concentration increased over 180 [mg/dL] and was rising,

**3)** The blood glucose concentration was predicted to drop lower than 80 [mg/dL] within the next 15 minutes.

Note that since the blood glucose concentration increases after a meal, no optimization was performed within the two hours following a meal insulin bolus. An exception was a too low blood glucose concentration.

The amounts of insulin and glucose determined by the optimization (5.3) were applied to the virtual patient. Moreover, they were applied to the prediction algorithm. In this way, future predictions take past glucose as well as insulin intakes into account. Hence, the blood glucose predictions $\hat{y}$ included information about the effect of past insulin intakes on the future blood glucose concentration. Through the predictions, the optimization problem within the controller had access to this information and could determine new intakes accordingly.

# 6

# Diabetic Glycemia Control via Selection

The approach used for the control algorithm proposed in this chapter was based on selecting doses of insulin and glucose to be applied to the diabetic patient from given sets. The criteria for selection was an asymmetric cost function.

To model the patient dynamics, the state-space model from Eq. (4.1) was used. This model had the rates of appearance of insulin and glucose as inputs, while the sets contained insulin and glucose doses. Hence, the doses of insulin and glucose were recalculated into their rates of appearance.

Using the rates of appearances, the patient model (4.1) and predictions of the blood glucose concentration described in Sec. 4.2, the asymmetric cost function was evaluated for every combination of insulin and glucose intakes from the given sets. The combination leading to the smallest cost was then applied to the virtual patient.

## 6.1  Predictions

The control algorithm proposed in this chapter used blood glucose predictions as they were calculated in Sec. 4.2. There, the blood glucose concentration was predicted employing past input and output data. However, it did not include the effect that insulin and glucose intakes suggested by a control algorithm within the prediction horizon have on the predicted blood glucose concentration. This effect has to be added to the predicted

blood glucose concentration for the control algorithm presented in this chapter.

The patient model (4.1) had rates of appearance as inputs, while the doses of insulin and glucose were to be compared using the asymmetric cost function. Hence, the insulin and glucose doses from the given sets were recalculated into their rates of appearance with Eq. (3.9) and Eq. (3.4), respectively. The rate of appearance of glucose at time $k$ is denoted by $u_{RA}^{(1)}(k)$ and the rate of appearance of insulin at time $k$ by $u_{RA}^{(2)}(k)$. Both rates of appearance were collected into one vector $u_{RA}(k) = [u_{RA}^{(1)}(k) \; u_{RA}^{(2)}(k)]^T$, which was the input vector for the patient model (4.1).

The input vector was then further divided into the rate of appearance from a meal and the rates of appearance from insulin and glucose intakes to be suggested by the control algorithm, see Eq. (6.1).

$$u_{RA}(k) = \begin{pmatrix} \bar{u}_{RA}^{(1)}(k) \\ 0 \end{pmatrix} + \begin{pmatrix} \tilde{u}_{RA}^{(1)}(k) \\ \tilde{u}_{RA}^{21)}(k) \end{pmatrix} \qquad (6.1)$$
$$= \bar{u}_{RA}(k) + \tilde{u}_{RA}(k)$$

The rate of appearance of glucose from a meal input is denoted by $\bar{u}_{RA}^{(1)}(k)$ and the rate of appearance from a glucose intake suggested by the control algorithm by $\tilde{u}_{RA}^{(1)}(k)$. Similarly, $\tilde{u}_{RA}^{(2)}(k)$ is the rate of appearance of insulin from an insulin intake suggested by the controller. Furthermore, it is $\bar{u}_{RA}(k) = [\bar{u}_{RA}^{(1)}(k) \; 0]^T$ and $\tilde{u}_{RA}(k) = [\tilde{u}_{RA}^{(1)}(k) \; \tilde{u}_{RA}^{(2)}(k)]^T$.

Denoting the blood glucose concentration at the output of the model in Eq. (4.1) at time $k$ with $y_s(k)$, the blood glucose concentration $p$ time steps ahead is, similarly as in Sec. 4.2, as shown in Eq. (6.2).

$$y_s(k+p) = CA^p x(k) + \sum_{m=0}^{p-1} CA^{p-1-m}B \; u_{RA}(k+m) \qquad (6.2)$$

The matrices of the state-space model (4.1) are denoted by $A$, $B$ and $C$. The state $x(k)$ is estimated using a Kalman filter.

Dividing the input $u_{RA}(k+m)$ as in Eq. (6.1) leads to Eq. (6.3).

$$y_s(k+p) = CA^p x(k) + \sum_{m=0}^{p-1} CA^{p-1-m} B \, \bar{u}_{RA}(k+m) \qquad (6.3)$$

$$+ \sum_{m=0}^{p-1} CA^{p-1-m} B \, \tilde{u}_{RA}(k+m)$$

The first two parts of the sum on the right hand side are the predicted output $\hat{y}(k+p)$, which the prediction algorithm in Sec. 4.2 calculates, so that

$$y_s(k+p) = \hat{y}(k+p) + \sum_{m=0}^{p-1} CA^{p-1-m} B \, \tilde{u}_{RA}(k+m) \qquad (6.4)$$

$$(6.5)$$

Since $\tilde{u}_{RA}(k) = [\tilde{u}_{RA}^{(1)}(k) \; \tilde{u}_{RA}^{(2)}(k)]^T$ and $B = [B_1 \; B_2]$, the sum in Eq. (6.4) can be separated into the effect of glucose and insulin on the future blood glucose, as shown in Eq. (6.6).

$$y_s(k+p) = \hat{y}(k+p) + \sum_{m=0}^{p-1} CA^{p-1-m} B_1 \, \tilde{u}_{RA}^{(1)}(k+m) \qquad (6.6)$$

$$+ \sum_{m=0}^{p-1} CA^{p-1-m} B_2 \, \tilde{u}_{RA}^{(2)}(k+m)$$

Collecting the future blood glucose values $y_s(k+p)$ for $p = 1, ..., H_p$ in a vector results in Eq. (6.7).

$$\mathcal{Y}_{s,H_p} = \hat{\mathcal{Y}}_{H_p} + \mathcal{S}_{u,1} \tilde{\mathcal{U}}_{1,H_p} + \mathcal{S}_{u,2} \tilde{\mathcal{U}}_{2,H_p} \qquad (6.7)$$

The vector of blood glucose predictions over the prediction horizon $H_p$ as in Eq. (4.3) is denoted by $\hat{\mathcal{Y}}_{H_p}$. It is provided by the prediction algorithm described in Sec. 4.2. The rates of appearance of glucose and insulin to be suggested by the control algorithm over the prediction horizon are $\tilde{\mathcal{U}}_{1,H_p}$

and $\tilde{\mathcal{U}}_{2,H_p}$, respectively. The matrices $\mathcal{S}_{u,1}$ and $\mathcal{S}_{u,2}$ are, for $i = 1, 2$,

$$
\mathcal{S}_{u,i} = \begin{pmatrix}
CB_i & 0 & 0 & \dots & 0 \\
CAB_i & CB_i & 0 & \dots & 0 \\
\vdots & \vdots & \ddots & \ddots & \vdots \\
CA^{H_p-1}B_i & CA^{H_p-2}B_i & \dots & CB_i & 0 \\
CA^{H_p}B_i & CA^{H_p-1}B_i & \dots & CAB_i & CB_i
\end{pmatrix}
$$

To test different combinations of insulin and glucose doses, Eq. (6.7) was used to calculate the blood glucose prediction within the prediction horizon for the insulin and glucose doses to be tested. As described in the next section, this will be used to evaluate which insulin and glucose doses lead to a minimum value of the asymmetric cost function from Sec. 5.1.

## 6.2  The Selection-based Control Algorithm

In the initialization phase of the control algorithm, some matrices and vectors were calculated in advance. The matrices $\mathcal{S}_{u,1}$ and $\mathcal{S}_{u,2}$ could be calculated in the initialization phase, since they depend on the patient model and not on the insulin and glucose doses to be given. Moreover, $\mathcal{S}_{u,1}\tilde{\mathcal{U}}_{1,H_p}$ and $\mathcal{S}_{u,2}\tilde{\mathcal{U}}_{2,H_p}$ were calculated in advance for all combinations of glucose and insulin doses in the given sets and stored for later usage. Shifting the rates of appearance for the glucose and insulin intakes $\tilde{\mathcal{U}}_{1,H_p}$ and $\tilde{\mathcal{U}}_{2,H_p}$ $k$ time steps into the future corresponds to taking the glucose or insulin intakes $k$ time steps further into the future during the prediction horizon. For time shifts of $0, 10, 20, ..., H_p$ time steps into the prediction horizon, $\mathcal{S}_{u,1}\tilde{\mathcal{U}}_{1,H_p}$ and $\mathcal{S}_{u,2}\tilde{\mathcal{U}}_{2,H_p}$ were calculated as well, for all the insulin and glucose dose combinations in the given sets and stored for later usage.

Motivated by intensified therapy used in diabetes treatment [26], the insulin and glucose intakes were determined at mealtime and when the blood glucose concentration was predicted to fall under 80 [mg/dL]. The algorithm determining the insulin and glucose doses was implemented as follows. For all insulin and glucose doses in the given sets and the time shifts to be tested, the asymmetric cost function in Eq. (6.8) was evaluated

and stored.

$$J = \sum_{k=0}^{H_p} [a \cdot y_s(k) + b + c \cdot \max\{(d - y_s(k))^3, 0\}] \qquad (6.8)$$
$$+ c_3||a_i||^2 + c_4||a_g||^2$$

Here, the blood glucose concentration $k$ time steps into the prediction horizon $y_s(k)$ is the $k$-th entry of the vector $\mathcal{Y}_{s,H_p}$ in Eq. (6.7), with $\mathcal{S}_{u,1}\tilde{\mathcal{U}}_{1,H_p}$ and $\mathcal{S}_{u,2}\tilde{\mathcal{U}}_{2,H_p}$ taken from the stored data according to the insulin and glucose doses and the time shifts to be tested. The value of the cost function (6.8) for all the tested doses and time shifts was compared, and the insulin and glucose doses and the time shifts leading to the smallest $J$ were chosen to be applied to the virtual patient.

# 7

# Simulations

In order to test and evaluate the proposed control algorithms in a closed-loop manner, the virtual patient described in Sec. 3 was used. The control algorithms, the predictor and the virtual patient were implemented in Matlab Simulink [47].

In this chapter, the simulation setup for both control algorithms is presented. Furthermore, a bolus calculator formula from the literature is described. The bolus calculator is used to compare the two control algorithms proposed in this thesis to. Moreover, the results of the simulations are given.

## 7.1 Simulation Setup for the Optimization-based Controller

The simulation setup used for the optimization-based controller described in Ch. 5 is shown in Fig. 7.1. The virtual patient takes glucose $u_g(t)$ and insulin $u_i(t)$ as inputs and gives out the blood glucose concentration signal $y_{BG}(t)$. All these signals are used by a prediction algorithm to predict the measured blood glucose concentration over a future horizon. The predictor uses a linear model of the patient, here a virtual patient, and a Kalman filter to calculate the predictions, see Sec. 4.2. The predictions of the blood glucose concentration and the blood glucose concentration at the output of the virtual patient are used by the optimization-based control algorithm to determine the doses of insulin and glucose to be given to the virtual patient, as described in Ch. 5.
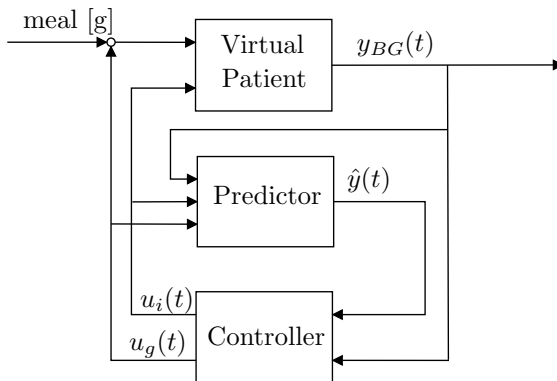
**Figure 7.1**    The simulation set-up.

The parameters to be set within the control algorithm are the weights $c_3$ and $c_4$, which punish the norm of the insulin and glucose dose sizes in the optimization problem (5.3). Table 7.1 shows these parameters for the virtual patients.

**Table 7.1**    Parameters used for the optimization-based controller presented in chapter 5

| Virtual Patient | $c_3$ | $c_4$ |
|:---:|:---:|:---:|
| 1 | 0 | 0 |
| 2 | 100 | 10 |
| 3 | 60 | 70 |

The algorithm was first tested without constraints on insulin and glucose intakes to test the ability of the controller to keep the blood glucose concentration in the safe range of $70 - 180$ [mg/dL]. Furthermore, the control algorithm was tested with constraints on insulin intakes to reduce the amount of glucose and insulin given to the patient per day.

## 7.2  Simulation Setup for Selection-based Controller

The setup used to simulate the controller presented in Chapter 6 is shown as well in Fig. 7.1. The prediction of the blood glucose concentration $\hat{y}(t)$ as well as the blood glucose concentration at the output of the virtual patient $y_{BG}(t)$ were inputs to the control algorithm. The outputs of the control algorithm were the determined glucose and insulin doses. The doses and times tested for insulin were $[1, 2, 3, ..., 20]$ at $[0, 10, 20, ..., H_p]$ time points after the optimization was called. For glucose the tested doses were $[10, 20, 30, ..., 80]$ at $[0, 10, 20, ..., H_p]$ time points after the optimization was called. The prediction horizon was $H_p = 180$.

The parameters $c_3$ and $c_4$ punishing the size of the insulin doses in the cost function (6.8) are shown in table 7.2.

**Table 7.2**   Parameters used for the selection-based controller

| Virtual Patient | $c_3$ | $c_4$ |
|:---:|:---:|:---:|
| 1 | 0.1 | 5 |
| 2 | 1 | 10 |
| 3 | 10 | 10 |

## 7.3  Simulation Setup for the Bolus Calculator

To compare the performance of the control algorithms presented in this thesis, an insulin bolus calculation formula as described in [62], [52] or [63] is used to determine the amount of insulin to be taken with meals. As shown in Eq. (7.1), this formula uses the current measured blood glucose concentration $y_{BG}$ of the virtual patient, the amount of carbohydrates in the meal $M$ [g] and a reference blood glucose concentration $y_r$, here $y_r = 126$ [mg/dL], to determine the meal insulin bolus.

$$u_{i,BC} = \frac{M}{c_{ITC}} + \frac{y_{BG} - y_r}{c_{ISF}} \tag{7.1}$$

The patient's insulin-to-carbohydrate ratio $c_{\text{ITC}}$ [g/IU] and insulin sensitivity factor $c_{\text{ISF}}$ [mg/dL/IU] can be determined using the total dose of insulin $c_{\text{TDD}}$ a patient takes per day through $c_{\text{ITC}} = 500/c_{\text{TDD}}$ and $c_{\text{ISF}} = 1800/c_{\text{TDD}}$ [64], [65]. If the total dose of insulin per day for a patient is not known through previous treatment, as it is the case for the virtual patients here, it can be approximated using $c_{\text{TDD}} = 0.66 \cdot W_{\text{body}}$, where $W_{\text{body}}$ is the patient's body weight in [kg] [64].

## 7.4 Evaluation Methods

To evaluate the glycemic control for the different control algorithms presented and compare them, the low blood glucose and high blood glucose indices as presented in [60], [66], [7] and the percentage of time spent in the normal blood glucose range of 70 to 180 [mg/dL] $T_{\text{safe}}$[%] are used.

The low blood glucose index (LBGI) and high blood glucose index (HBGI) evaluate the glycemic control of a diabetic patient considering the risk for hypoglycemia and hyperglycemia, respectively [60]. The LBGI gives a measure of the frequency and magnitude of low blood glucose readings, while the HBGI gives a measure of the frequency and magnitude of high blood glucose readings [66]. They are calculated based on a risk function, which emphasizes the higher risk connected to low blood glucose readings compared to high blood glucose readings. This risk function is given in Eq. (7.2) [66], [7].

$$r(y_{\text{BG}}) = 10 \cdot f(y_{\text{BG}})^2 \tag{7.2}$$
$$f(y_{\text{BG}}) = 1.509 \cdot ((\ln(y_{\text{BG}}))^{1.084} - 5.381)$$

The left branch $r_l(y_{\text{BG}})$ of the risk function (7.2) is connected to the risk for hypoglycemia and its right branch $r_h(y_{\text{BG},i})$ to the risk of hypoglycemia. These branches are calculated as given in Eq. (7.3) [66], [7].

$$r_l(y_{\text{BG}}) = \begin{cases} r(y_{\text{BG}}) & f(y_{\text{BG}}) < 0 \\ 0 & \text{otherwise} \end{cases} \tag{7.3}$$
$$r_h(y_{\text{BG}}) = \begin{cases} r(y_{\text{BG}}) & f(y_{\text{BG}}) > 0 \\ 0 & \text{otherwise} \end{cases}$$

With this, the LBGI and HBGI are calculated as stated in Eq. (7.4) [66], [7].

$$\text{LBGI} = \frac{1}{n} \sum_{i=1}^{n} r_l(y_{\text{BG},i}) \tag{7.4}$$

$$\text{HBGI} = \frac{1}{n} \sum_{i=1}^{n} r_h(y_{\text{BG},i})$$

In order to avoid both hypoglycemia and hyperglycemia, both LBGI and HBGI should be small. According to [66], patients can be classified according to the clinical risk connected to their measured blood glucose concentration into three zones representing low, medium and high risk for hypoglycemia and hyperglycemia for both LBGI and HBGI, as shown in Table 7.3.

**Table 7.3**   Clinical risk of a a measured blood glucose concentration obtained through LBGI and HBGI, to classify the quality of the glycemic control [66].

| | | **HBGI** | | |
|---|---|---|---|---|
| | | **< 5.4** | **4.5 − 9** | **> 9** |
| **LBGI** | **< 2.5** | low (L) | low/medium (L/M) | low/high (L/H) |
| | **2.5 − 5** | medium/low (M/L) | medium (M) | medium/high (M/H) |
| | **> 5** | high/low (H/L) | high/medium (H/M) | high (H) |

## 7.5  Simulation Results

The simulation results of the control algorithms described in the previous chapters are presented here. Figures showing the results including the measured blood glucose concentration, the amount of carbohydrates in the meals and the advice given by the controllers are shown in Appendix

**Table 7.4**    Result Summary for Virtual Patient 1.
BC (Bolus Calculator), Opt (Optimization), SelC (Selection Controller); LBGI (low blood glucose index), HBGI (high blood glucose index), clin. risk (clinical risk according to Table 7.3), $I_{\sum}$ (total daily insulin dose), $G_{\sum}$ (total daily carbohydrate consumption, without meals)

|      | LBGI | HBGI  | clin. risk | $T_{safe}[\%]$ | $I_{\sum}$ [U] | $G_{\sum}$ [g] |
|------|------|-------|------------|----------------|----------------|----------------|
| BC   | 0    | 12.59 | L/H        | 53             | 17.2           | 0              |
| Opt  | 0.22 | 3.59  | L          | 85             | 85.7           | 152.3          |
| SelC | 0.37 | 2.97  | L          | 82             | 20.01          | 20.01          |

**Table 7.5**    Result Summary for Virtual Patient 2.
BC (Bolus Calculator), Opt (Optimization), SelC (Selection Controller); LBGI (low blood glucose index), HBGI (high blood glucose index), clin. risk (clinical risk according to Table 7.3), $I_{\sum}$ (total daily insulin dose), $G_{\sum}$ (total daily carbohydrate consumption, without meals)

|      | LBGI | HBGI | clin. risk | $T_{safe}[\%]$ | $I_{\sum}$ [U] | $G_{\sum}$ [g] |
|------|------|------|------------|----------------|----------------|----------------|
| BC   | 0.19 | 2.66 | L          | 87             | 17.6           | 0              |
| Opt  | 0.35 | 1.11 | L          | 100            | 34.5           | 136.5          |
| SelC | 0.45 | 1.90 | L          | 93             | 18.01          | 20.01          |

B. A summary of the results using LBGI, HBGI, percent of time in safe rage $T_{safe}[\%]$, total amount of insulin dose advice per day $I_{\sum}$ and the total amount of glucose dose advice $G_{\sum}$ is shown in the tables 7.4, 7.5 and 7.6. Each row of the tables shows the results for one of the control algorithms. The bolus calculator described in Sec. 7.3 is denoted by BC, the optimization-based controller from Ch. 5 by Opt and the selection-based controller from Ch. 6 by SelC.

The goal for the HBGI and LBGI is to have them as low as possible (compare to Sec. 7.4), where the clinical risk connected to the HBGI and LBGI as shown in Table 7.3 helps for the evaluation of these two indices. Furthermore, the time $T_{safe}[\%]$ spent in safe blood glucose range and the

**Table 7.6** Result Summary for Virtual Patient 3.
BC (Bolus Calculator), Opt (Optimization), SelC (Selection Controller); LBGI (low blood glucose index), HBGI (high blood glucose index), clin. risk (clinical risk according to Table 7.3), $I_{\sum}$ (total daily insulin dose), $G_{\sum}$ (total daily carbohydrate consumption, without meals)

|      | LBGI | HBGI | clin. risk | $T_{\text{safe}}$[%] | $I_{\sum}$ [U] | $G_{\sum}$ [g] |
|------|------|------|------------|------------------|------------|------------|
| BC   | 0.47 | 4.45 | L          | 76               | 13.8       | 0          |
| Opt  | 0.25 | 2.61 | L          | 80               | 42.6       | 172.3      |
| SelC | 0.37 | 2.97 | L          | 82               | 20.01      | 20.01      |

total daily insulin and glucose dose advices are supposed to be low as well.

For all three tested virtual patients, the optimization-based control algorithm Opt presented in Ch. 5 achieved a lower LBGI and HBGI than the bolus calculator, which implies a lowered risk for low and high blood glucose values. Furthermore, the percent of time spent in the safe range $70 - 180$ [mg/dL] was higher than the bolus calculator for all tested virtual patients. This decreased risk for blood glucose values outside the safe range had to be paid for by increased doses of insulin and glucose. For an example patient, the simulation results obtained with the bolus calculator are shown in Fig. 7.2 and those obtained with the optimization-based controller are shown in Fig. 7.3. In this case, the amount of insulin for the optimization-based controller was not constrained. As can be seen in Fig. 7.2, the bolus calculator determined insulin doses bringing the blood glucose concentration back into safe range after a meal. However, it is conservative concerning the size of the insulin doses, leading to a shorter time in safe range than for the optimization-based controller. The results for the optimization-based controller in Fig. 7.3 show that without further restrictions of the size of the insulin and glucose doses, the controller was more aggressive than the bolus calculator. Alongside with the counteracting carbohydrates, this leads to an increase of time spent in safe range compared to the bolus calculator, but also an increase in the amount of insulin and carbohydrates taken by the patient.

By constraining the amounts of insulin and glucose in the optimization problem, less insulin and glucose per day could be achieved. Table
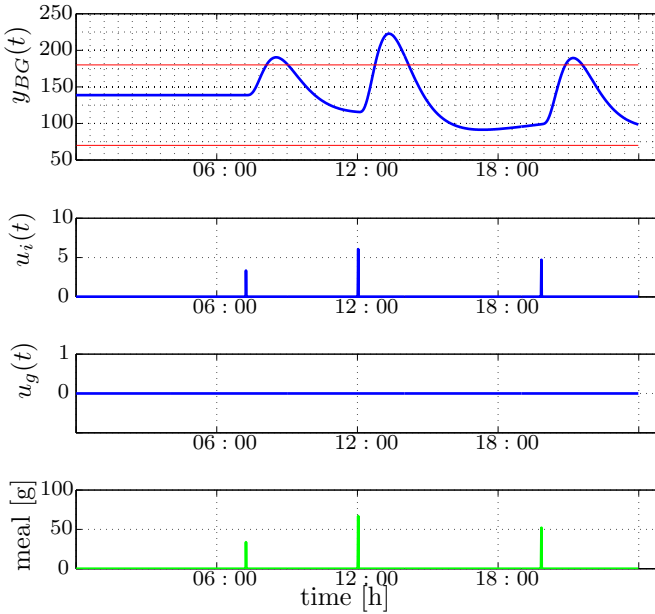
**Figure 7.2**    Simulation results for Virtual Patient 2 with Bolus Calculator.

7.7 shows results when the amount of insulin per injection were restricted to 15 units per intake for patient 1 and to 5 units per intake for patient 2 and patient 3. It can be seen that the amount of insulin and glucose per day was reduced, but the time in safe range $T_{safe}[\%]$ decreased and the HBGI increased, compare also to Fig. 7.3 and Fig. 7.5. Figure 7.3 shows the case when the amount of insulin per injection is not restricted, and Fig. 7.5 shows when it is restricted. When restricting the insulin dose, it seems from Fig. 7.5 that the behavior of the optimization-based control algorithm got closer to that of the bolus calculator. The optimization-based algorithm was still slightly more aggressive than the bolus calculator, and it had a longer residence time in the safe range. Similar results can be seen for other simulated patients, see Appendix B.

The control algorithm based on selection presented in Ch. 6 lead to a lower HBGI than the bolus calculator for all tested patients. Figure
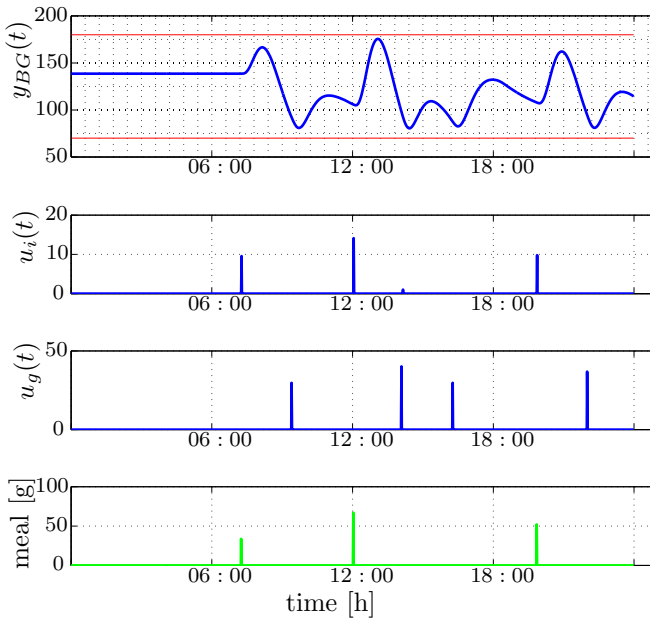
**Figure 7.3**  Simulation results for Virtual Patient 2 with the optimization-based controller, tuned for good control.

7.4 shows the simulation results for a sample patient with the selection-based controller. For two out of three patients, the HBGI was slightly higher than for the selection-based controller. This can also be seen by comparing Fig. 7.4 and Fig. 7.2. As the optimization-based controller, the selection-based controller spenf more time in safe range than the bolus caluclator. Comparing the amounts of glucose and insulin given to the patient with the selection-based controller to the amounts given with the optimization-based controller, it can be seen in the Tables 7.4, 7.5 and 7.6 that the selection-based controller gave significantly less insulin and glucose to the patient. Compared to the optimization-based controller with constrained insulin dose size, the selection-based controller spend more time in safe range, while still having comparibly low insulin and glucose doses per day.
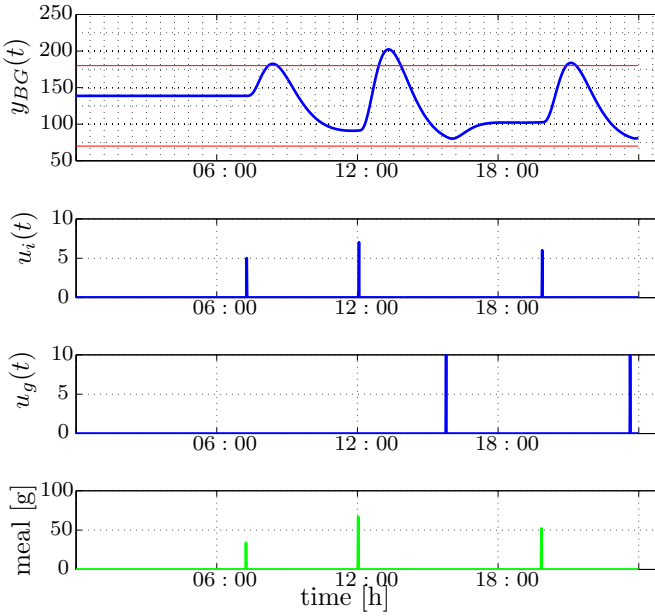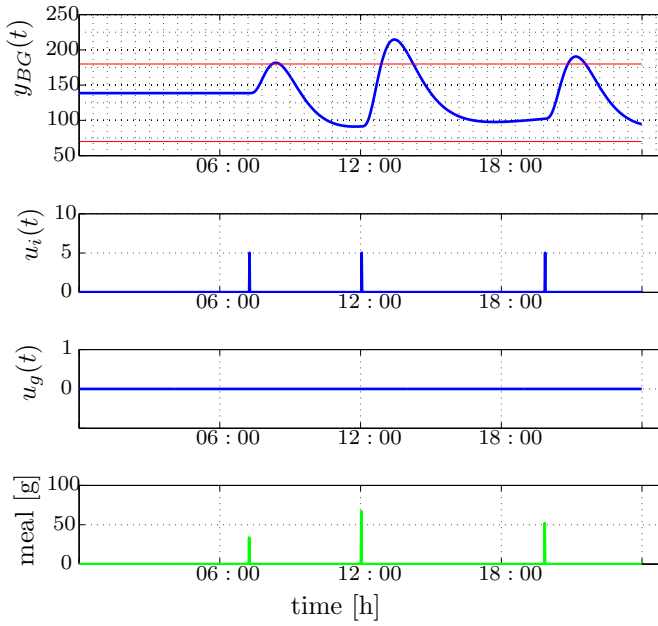
**Figure 7.4** Simulation results for Virtual Patient 2 with the selection-based controller

**Table 7.7** Results of the optimization-based controller, tuned to give less insulin and glucose dose advices. The amount of insulin has been constrained to 15 units for patient 1, 5 units for patient 2 and 5 units for patient 3; LBGI (low blood glucose index), HBGI (high blood glucose index), clin. risk (clinical risk according to Table 7.3), $I_{\sum}$ (total daily insulin dose), $G_{\sum}$ (total daily carbohydrate consumption, without meals)

|  | LBGI | HBGI | clin. risk | $T_{safe}[\%]$ | $I_{\sum}$ [U] | $G_{\sum}$ [g] |
|---|---|---|---|---|---|---|
| Pat 1 | 0.28 | 5.36 | L | 78 | 47.85 | 24.68 |
| Pat 2 | 0.20 | 2.32 | L | 90 | 15.01 | 0 |
| Pat 3 | 0.17 | 4.27 | L | 76 | 15.01 | 16.31 |

**Figure 7.5**   Simulation results for Virtual Patient 2 with the optimization-based controller, tuned for less insulin and glucose dose advice.

# 8

# Discussion

In order to help diabetic patients using multiple insulin intakes per day, the intention was to develop an algorithm calculating insulin and glucose dose advices using optimization methods. The goal was to spend as much time as possible to the target blood glucose range of $70 - 180$ [mg/dL], while avoiding hyperglycemia and, more importantly, hypoglycemia (see Sec. 1.2).

In this thesis, two different control algorithms have been proposed, which gave both insulin and additional glucose dose advice. It was assumed that the basal insulin need was covered. Hence, the control algorithms determined insulin needs at mealtimes. Furthermore, glucose dose intakes were determined in case of too low blood glucose concentration.

For evaluation, the proposed algorithms were compared to a bolus calculator as found in e.g. [62], [52] or [63].

As shown in the Tables 7.4, 7.5 and 7.6, the risk for low and high blood glucose values could be reduced using the optimization-based control algorithm presented in Ch. 5. On the other hand, the reduced risk came with an increase of the amount of insulin and glucose to be taken by the patient. This result is not surprising, since the objective function of the optimization problem did not include penalty on the dose sizes.

As shown in Table 7.7, the optimization-based control algorithm could be tuned to give less insulin and glucose to the diabetic patient. However, this led to a decreased control performance, i.e., less time in safe range and a higher HBGI. With the limited insulin and glucose amounts, for two out of the three patients the time in safe range was still higher than for the bolus calculator, and in none of the cases did the performance get

worse than the bolus calculator.

The selection-based controller SelC did not have any constraints on the optimization variabels or the blood glucose concentration at the output of the virtual patient. It based its decision about the insulin and glucose doses only on the cost function. Even without constraining the allowed insulin and glucose dose sizes, the selection-based controller could reach a higher time in safe range $T_{safe}[\%]$ than the bolus calculator and a lower HBGI while giving significantly smaller insulin and glucose doses than the optimization-based controller. In comparison to the optimization-based controller with constraints on the size of the insulin doses, the selection-based controller had a longer residence time in safe range, while still keeping comparably low insulin and glucose doses.

In order to have good glycemic control, the absorption of carbohydrates into the blood should be matched by the absorption profile of insulin into the bloodstream to even out the blood glucose concentration [67]. Because of delays in the insulin absorption, this is not the case when injecting insulin externally. To reduce the increase of blood glucose after a meal, larger amounts of insulin had to be given, increasing the risk for hypoglycemia. According to [26], intensified therapy of diabetes leads to an increased risk for hypoglycemia. The results presented in Ch. 7 and also in the Appendix B show that by giving more insulin than the bolus calculator did, the optimization-based algorithm could decrease glucose excursions after meals and the time spent outside safe range. However, in order to avoid hypoglycemia large amounts of extra carbohydrates had to be given to the patient in case of larger insulin intakes. Furthermore, when restricting the amount of insulin that the optimization-based algorithm was allowed to give to the patient per injection, the amount of insulin per day and as a result also the amount of extra glucose per day could be decreased. With these results it seemed there was a trade-off to be made between the blood glucose concentration being in safe range as long as possible and restricting the amount of insulin and glucose to be taken by the patient. In the optimization-based control algorithm, adjusting parameters and constraints on insulin and glucose intakes could be used to tune the trade-off and to adjust the aggressiveness of the controller, which influences the time spent in safe range.

It can be seen in the figures shown in Ch. 7 and in Appendix B that the optimization-based and the selection based control algorithms keep away from hypoglycemia for all tested patients. This is due to the fact that

the amounts of insulin and glucose doses were determined when the blood glucose concentration was predicted to drop under 80 [mg/dL] within the next 15 minutes. This allows for time to react before the blood glucose drops too low.

The approach in this thesis was to give advices for single insulin injections. Compared to a bolus calculator (see Sec. 7.3), the approaches here aimed at improving glycemic control by including more knowledge about the specific patient than the bolus calculator through an individual patient model in the control algorithm. A mathematical patient model enabled predictions of future blood glucose concentration to be made. These predictions allowed the controller to take the expected future development of the blood glucose concentration and the future expected impact of insulin and glucose intakes into account when making its decisions. This gave the chance for a higher degree of individualization than with the bolus calculator. Although estimating good patient models from real patient data remains challenging [50], such a model could describe the patient dynamics, and thus how a specific patient's blood glucose concentration reacts to intakes of insulin and glucose, in greater detail than the parameters used in a simple bolus calculation algorithm.

The optimization-based controller used patient models, which had the doses of insulin and glucose as inputs. Here, the model parameters were estimated from virtual patient data, where the input signals could be chosen with some freedom in order to provide sufficient excitation to the system to be estimated. However, this freedom is restricted when these models are to be estimated from clinical patient data. Hence, estimating a good patient model is more problematic. On the other hand, the selection-based controller uses state-space models having insulin and glucose rates of appearance as inputs, which are less problematic to estimate. In [50], ARMAX models with insulin and glucose rates of appearance were estimated for real patient data.

It can be seen in the figures shown in the Appendix B, that the bolus calculator in general gave smaller insulin doses than the optimization-based controller, in order to safely stay away from hypoglycemia. For patient 2 however, the last insulin dose lead to hypoglycemia. By predicting the effect of an insulin or glucose intake on the blood glucose concentration, the controller had the chance to keep the blood glucose concentration in tighter bounds. Hence, as seen in the results for the optimization-based controller, the control algorithm suggested the administration of larger

insulin doses. Furthermore, the prediction of the blood glucose concentration enabled the control algorithm to suggest counteracting carbohydrates before the blood glucose concentration falls under 80 [mg/dL], so that hypoglycemia could be prevented.

Through the mathematical model and the prediction algorithm, the ongoing effect of past insulin intakes on the blood glucose concentration was already included in the control algorithm. If insulin was taken in the past, the blood glucose concentration would be predicted to decrease. This blood glucose prediction was used by the optimization algorithm to determine a new insulin dose. Using a bolus calculator, this would have to be added extra as an insulin-on-board module in order to prevent stacking of insulin intakes. Furthermore, it would be possible to include the effect of future meals on the blood glucose concentration by using a mathematical model and a prediction algorithm.

The optimization problem formulated to determine the insulin and glucose doses did not have output constraints, since it was found that introducing constraints of $70 - 180$ [mg/dL] on the output lead to infeasibility problems when solving the optimization problem. A meal would unavoidably increase the blood glucose concentration to rise over 180 [mg/dL]. A small dose of insulin taken to cover the meal would lead to a blood glucose concentration that still rises over 180 [mg/dL] within the first 1-2 hours after the meal, making the optimization algorithm infeasible. If this increased blood glucose concentration could be avoided by overdosing insulin, the blood glucose concentration would fall below 70 [mg/dL] within the prediction horizon, leading to infeasibility as well. A way around this infeasibility problem could be to introduce output constraints with dynamically adjusted size depending on meal size, within the first 2 hours after a meal. However, it was found in this thesis that good results could be achieved even without the use of output constraints.

Even though it still remained to be tested how the optimization-based control algorithm presented in this thesis performs compared to a bolus calculator in the presence of disturbances like stress or exercise, using optimization algorithms and blood glucose predictions to decide upon insulin and glucose intakes has been found to improve glucose control compared to a bolus calculator in simulation-based tests. Through the use of mathematical models, more detailed knowledge about the patient dynamics could be incorporated into the algorithm than a bolus calculator does.

Looking back at the goal formulated in Sec. 1.2, the time spent in the safe glycemic range could be increased for the optimization-based and the selection-based control algorithms proposed in this thesis, as compared to a bolus calculator algorithm found in literature, for all virtual patients tested here. While the bolus calculator reached maximum 87 % time in safe range and even as low as 53 %, the optimization-based algorithm could reach between 80 and 100 % time in safe range and the selection-based control algorithm between 82 % and 93 %, depending on the individual patient.

# 9

# Conclusion and Future Work

In order to give advice about insulin intakes to diabetic patients, where the insulin dose advice should be a pulse-shaped signal, a mathematical optimization problem was proposed to determine insulin intake at mealtime and extra insulin and glucose intakes when the blood glucose concentration leaves the range of $70 - 180$ [mg/dL]. The control algorithm that incorporated this optimization problem used predictions of future blood glucose concentration, which were determined by a prediction algorithm based on past and present blood glucose measurements and insulin and glucose intakes. The optimization problem as well as the prediction algorithm made use of mathematical models describing the dynamics of a diabetic patient. The control algorithm was tested in simulations using a virtual implementation of a diabetic patient.

Moreover, a bolus calculator algorithm from literature was implemented to compare the results obtained with the proposed control algorithm. It was found that using mathematical optimization, the time in the safe range of $70 - 180$ [mg/dL] could be increased compared to the bolus calculator for all tested patients, but at the cost of increased amounts of insulin and glucose intakes. The proposed algorithm could avoid hypoglycemia in all cases.

The optimization-based control algorithm could be tuned such that the amounts of insulin and glucose given to the diabetic patient were reduced. This results in less time spent in safe range and thus characteristics, which approached those of a bolus calculator.

However, careful tuning of the optimization-based control algorithm had the potential to improve glycemic control as compared to the bolus calculator.

The proposed algorithms provided freedom for individualization through individualized mathematical models and controller parameters, so that the controller could be adjusted specifically to the patient to be treated, to give individualized advice.

To improve the algorithm further, insulin intakes should be allowed before meal intake, since the dynamics of appearance of insulin into the blood stream are slower than the dynamics of appearance of glucose from a meal into the blood stream. Furthermore, it should be possible to determine additional glucose intakes at a later time point within the prediction horizon and not necessarily at the same time as the insulin intake.

Another approach could be to constrain the blood glucose concentration of the patient to, e.g., 140 [mg/dL] from two hour after a meal onward. The International Federation of Diabetes recommended that the two-hour postmeal blood glucose concentration should not exceed 140 [mg/dL], as long as hypoglycemia can be avoided [68].

# A

# Convexity of the Cost Function

One of the advantages of the cost function (5.1) over, e.g., the asymmetric cost presented in [60] is that it is convex. The convexity of $L(y(k))$ in Eq. (5.1) with respect to $y(k)$ can be shown as follows. First, it is shown that $L_1 = \max\{(d - y(k))^3, 0\}$ is convex in $y(k)$. It is $L_1 = \max\{(d - y(k))^3, 0\} = (\max\{(d - y(k)), 0\})^3$. Since $\max\{(d - y(k)), 0\}$ is the point wise maximum of two affine functions, it is convex. The function $x^3$ is convex and non-decreasing as long as $x \geq 0$. The composition of these two convex functions to $L_1 = (\max\{(d - y(k)), 0\})^3$, gives a convex function [61]. Note that $\max\{(d - y(k)), 0\}$ is always positive. The second part of $L(y(k))$, which is $L_2 = a \cdot y(k) + b$, is an affine function and thus convex. The weighted sum of $L_1$ and $L_2$ gives $L(y(k)) = L_2 + cL_1$, and is convex since $L_1$ and $L_2$ are convex and $c \geq 0$ [61].

# B

# Simulation Results
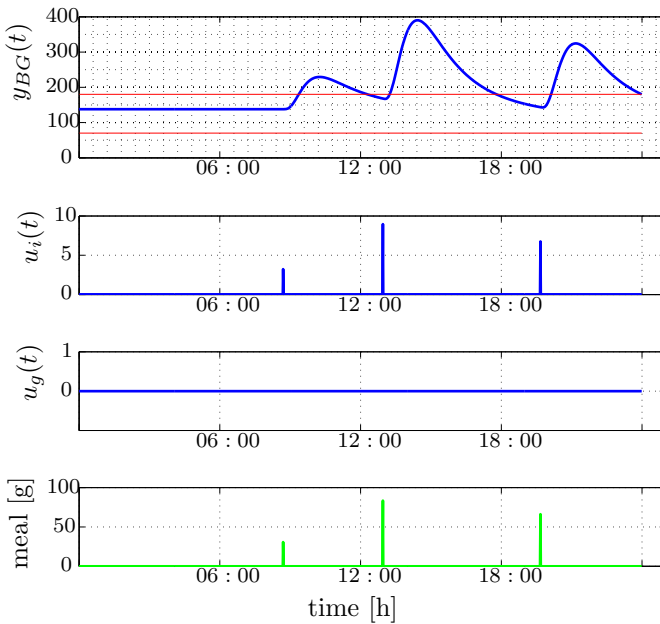


**Figure B.1**    Simulation results for Virtual Patient 1 with Bolus Calculator.
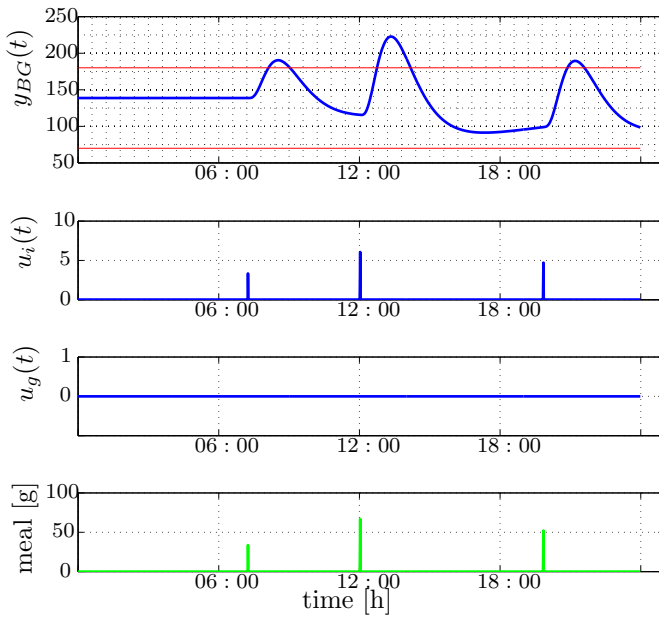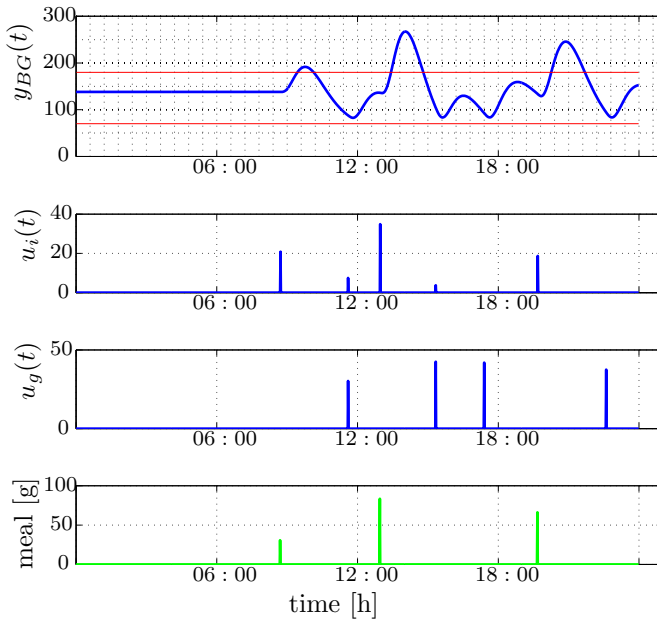
**Figure B.2**   Simulation results for Virtual Patient 2 with Bolus Calculator.
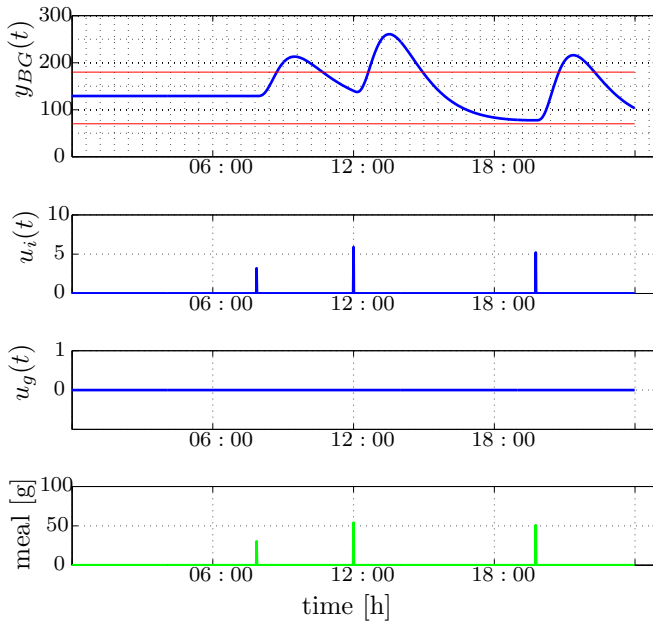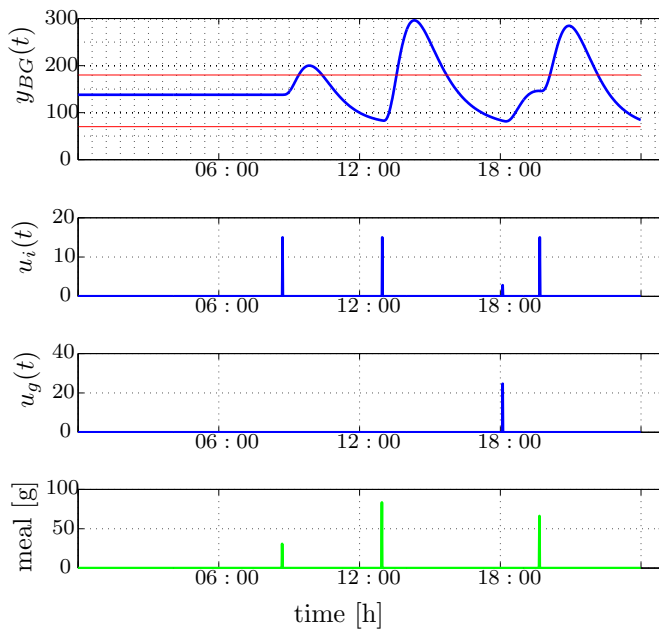
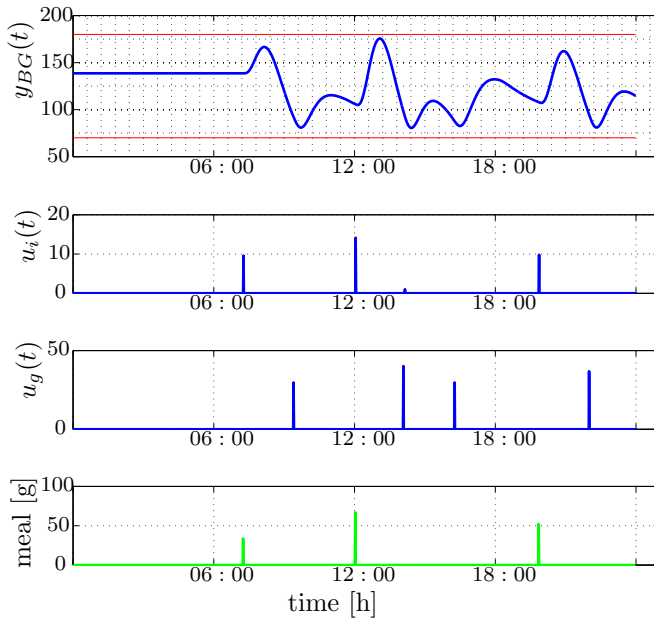**Figure B.3**  Simulation results for Virtual Patient 3 with Bolus Calculator.

**Figure B.4**    Simulation results for Virtual Patient 1 with the optimization-based controller, tuned for good control.
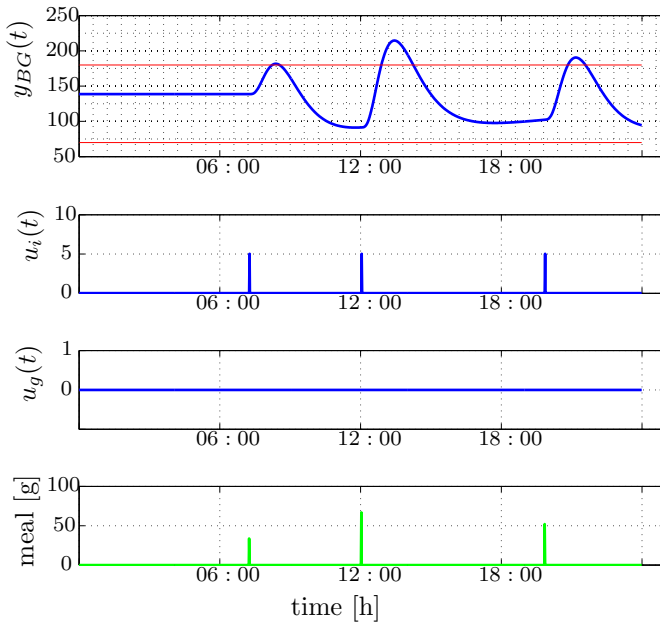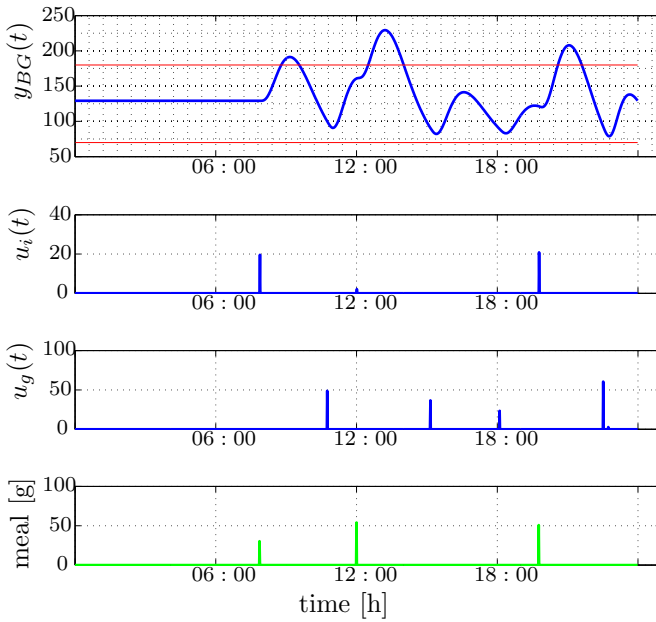
**Figure B.5** Simulation results for Virtual Patient 1 with the optimization-based controller, tuned for less insulin and glucose dose advices

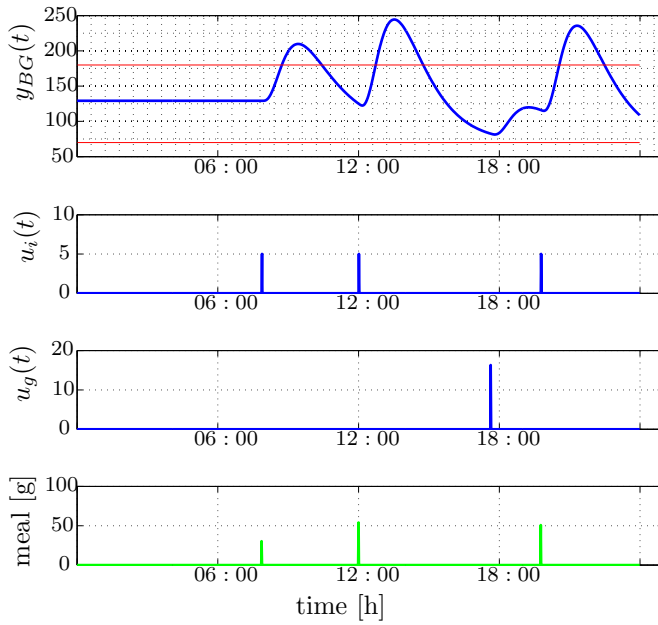**Figure B.6** Simulation results for Virtual Patient 2 with the optimization-based controller, tuned for good control.

**Figure B.7** Simulation results for Virtual Patient 2 with the optimization-based controller, tuned for less insulin and glucose dose advice.
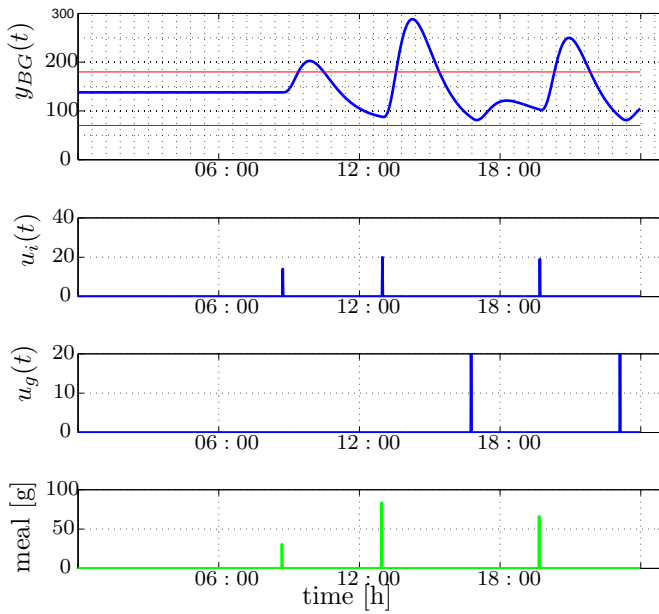
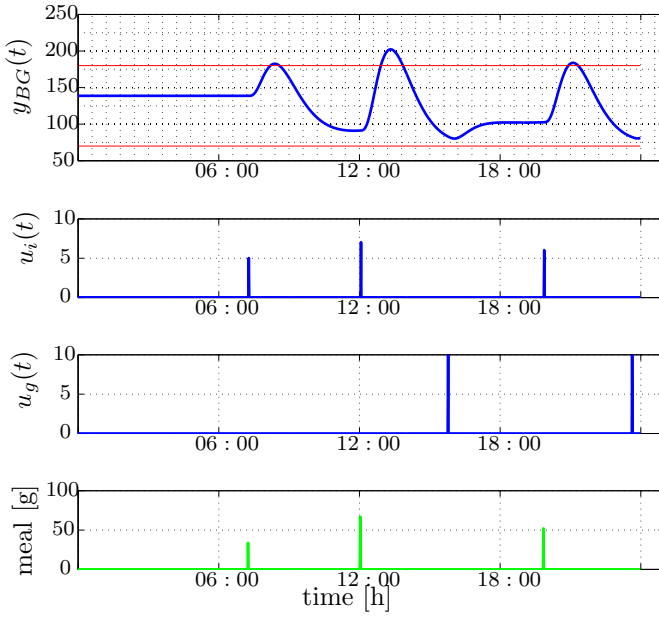**Figure B.8** Simulation results for Virtual Patient 3 with the optimization-based controller, tuned for good control.

**Figure B.9**  Simulation results for Virtual Patient 3 with the optimization-based controller,tuned for less insulin and glucose dose advice.
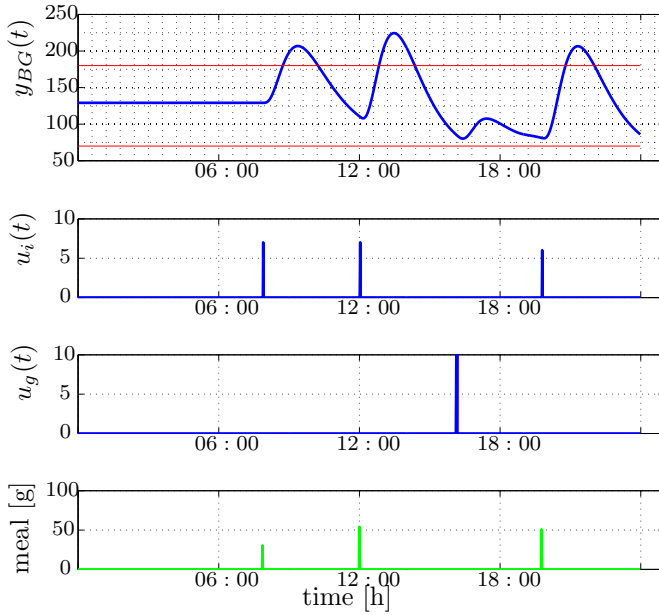
**Figure B.10**   Simulation results for Virtual Patient 1 with the selection based controller.

**Figure B.11**  Simulation results for Virtual Patient 2 with the selection based controller.

**Figure B.12** Simulation results for Virtual Patient 3 with the selection based controller.

# C

# Bibliography

[1] A. C. Guyton and J. E. Hall, "Textbook of medical physiology," ch. 78, Philadelphia, PA, USA: Elsevier Saunders, 11 ed., 2006.

[2] World Health Organization, "Diabetes programme." `http://www.who.int/diabetes/en/`. Accessed January 2013.

[3] International Federation of Diabetes, "IDF Diabetes Atlas, 2012 update." `http://www.idf.org/diabetesatlas/`, 2012.

[4] International Federation of Diabetes, "IDF Diabetes Atlas." `http://www.idf.org/diabetesatlas/`, 2011.

[5] F. Ståhl and R. Johansson, "Diabetes mellitus modeling and short-term prediction based on blood glucose measurements," *Mathematical Biosciences*, vol. 217, no. 2, pp. 101–117, 2009.

[6] M. Cescon, F. Stahl, M. Landin-Olsson, and R. Johansson, "Subspace-based model identification of diabetic blood glucose dynamics system identification," in *15th IFAC Symposium on System Identification (SYSID 2009)*, vol. 15, (Saint-Malo, France), July 2009.

[7] C. Cobelli, C. Dalla Man, G. Sparacino, G. De Nicolao, and B. Kovatchev, "Diabetes: Models, signals and control," *Biomedical Engineering, IEEE Reviews in*, vol. 2, pp. 54–96, 2009.

[8] R. Harvey, Y. Wang, B. Grosman, M. Percival, W. Bevier, D. Finan, H. Zisser, D. Seborg, L. Jovanovic, F. Doyle, and E. Dassau, "Quest for the artificial pancreas: Combining technology with treatment,"

*Engineering in Medicine and Biology Magazine, IEEE*, vol. 29, pp. 53–62, 2010.

[9] R. Parker, F. I. Doyle, and N. Peppas, "The intravenous route to blood glucose control," *Engineering in Medicine and Biology Magazine, IEEE*, vol. 20, pp. 65–73, 2001.

[10] J. U. Poulsen, A. Avogaro, F. Chauchard, C. Cobelli, R. Johansson, L. Nita, M. Pogose, L. del Re, E. Renard, S. Sampath, F. Saudek, M. Skillen, and J. Soendergaard, "A diabetes management system empowering patients to reach optimised glucose control: From monitor to advisor," in *2010 Annual International Conference of the IEEE Engineering in Medicine and Biology Society (EMBC 2010)*, (Buenos Aires , Argentina), pp. 5270 – 5271, August 31 - September 4 2010.

[11] "DIAdvisor." `http://www.diadvisor.org`. Accessed 2012-11-15.

[12] "The DIAdvisor consortium (2012): Final publishable summary report.." `http://cordis.europa.eu/results/home_en.html`. Accessed 2012-11-15.

[13] M. Cescon, M. Stemmann, and R. Johansson, "Impulsive predictive control of T1DM glycemia: An in-silico study," in *5th Annual Dynamic Systems and Control Conference (ASME 2012), Ft. Lauderdale, FL, USA*, October 17-19 2012.

[14] M. Stemmann and R. Johansson, "Control of type 1 diabetes via risk-minimization for multi dose injection patients," in *5th International Conference on Advanced Technologies and Treatments for Diabetes (ATTD 2012), Barcelona, Spain*, February 8-11 2012.

[15] M. Stemmann and R. Johansson, "Diabetic blood glucose control via optimization over insulin and glucose doses," in *8th IFAC Symposium on Biological and Medical Systems (IFAC BMS 2012), Budapest, Hungary*, August 29-31 2012.

[16] M. Stemmann, F. Stahl, J. Lallemand, E. Renard, and R. Johansson, "Sensor calibration models for a non-invasive blood glucose measurement sensor," in *2010 Annual International Conference of the IEEE Engineering in Medicine and Biology Society (EMBC 2010), Buenos Aires, Argentina*, pp. 4979–4982, August 31 - September 4 2010.

[17] M. Shrayyef and J. Gerich, "Normal glucose homeostasis," in *Principles of Diabetes Mellitus* (L. Poretsky, ed.), pp. 19–35, Springer, 2010.

[18] D. A. Warrell, T. M. Cox, and J. D. Firth, "Diabetes," in *Oxford Textbook of Medicine*, ch. 13.11.1, `oxfordmedicine.com/10.1093/med/9780199204854.001.1/med-9780199204854`: Oxford University Press, New York, NY, 2012.

[19] M. J. Fowler, "The Diabetes Treatment Trap," *Clinical Diabetes*, vol. 29, 2011.

[20] G. Williams and P. J.C., *Handbook of Diabetes*. Maldan, MA: Blackwell Science, 2 ed., 2001.

[21] M. J. Fowler, "Diabetes: Magnitude and Mechanisms," *Clinical Diabetes*, vol. 28, pp. 42–46, 2010.

[22] M. J. Fowler, "Diagnosis, Classification, and Lifestyle Treatment of Diabetes," *Clinical Diabetes*, vol. 28, pp. 79–86, 2010.

[23] F. G. Banting and C. H. Best, "The internal secretion of the pancreas," in *J Lab Clin Med*, pp. 251–266, 1922. [Reprinted in Vol. 80, 1972, to mark 50th anniversary of the discovery].

[24] M. J. Fowler, "Insulin and Incretins," *Clinical Diabetes*, vol. 26, pp. 35–39, 2008.

[25] I. Heukamp, C. Then, A. Lechner, and J. Seissler, "Update on type-1 diabetes.," *Internist (Berl)*, vol. 54, no. 2, pp. 201 – 216, 2012.

[26] D. R. Group *et al.*, "Diabetes control and complications trial (dcct): the effect of intensive treatment of diabetes on the development and progression of long-term complications in insulin dependent diabetes mellitus," *N Engl J Med*, vol. 329, no. 14, pp. 977–86, 1993.

[27] A. Albisser, B. Leibel, T. Ewart, Z. Davidovac, C. Botz, and W. Zingg, "An artificial endocrine pancreas," *Diabetes*, vol. 23, no. 5, pp. 389–396, 1974.

[28] E. Kraegen, L. Campbell, Y. Chia, H. Meier, and L. Lazarus, "Control of blood glucose in diabetics using an artificial pancreas*," *Australian and New Zealand Journal of Medicine*, vol. 7, no. 3, pp. 280–286, 1977.

[29] H. Connor, G. Atkin, and E. Attwood, "Short-term control of brittle diabetes using a biostator.," *British Medical Journal (Clinical research ed.)*, vol. 285, no. 6351, p. 1316, 1982.

[30] C. Cobelli, E. Renard, and B. Kovatchev, "Artificial pancreas: past, present, future," *Diabetes*, vol. 60, no. 11, pp. 2672–2682, 2011.

[31] G. Steil, K. Rebrin, C. Darwin, F. Hariri, and M. Saad, "Feasibility of automating insulin delivery for the treatment of type 1 diabetes," *Diabetes*, vol. 55, no. 12, pp. 3344–3350, 2006.

[32] G. Steil, A. Panteleon, and K. Rebrin, "Closed-loop insulin delivery—the path to physiological glucose control," *Advanced drug delivery reviews*, vol. 56, no. 2, pp. 125–144, 2004.

[33] S. Weinzimer, G. Steil, K. Swan, J. Dziura, N. Kurtz, and W. Tamborlane, "Fully automated closed-loop insulin delivery versus semi-automated hybrid control in pediatric patients with type 1 diabetes using an artificial pancreas," *Diabetes Care*, vol. 31, no. 5, pp. 934–939, 2008.

[34] A. Panteleon, M. Loutseiko, G. Steil, and K. Rebrin, "Evaluation of the effect of gain on the meal response of an automated closed-loop insulin delivery system," *Diabetes*, vol. 55, no. 7, pp. 1995–2000, 2006.

[35] R. Parker, J. Doyle III, J. Harting, and N. Peppas, "Model predictive control for infusion pump insulin delivery," in *Engineering in Medicine and Biology Society, 1996. Bridging Disciplines for Biomedicine. Proceedings of the 18th Annual International Conference of the IEEE*, vol. 5, (Amsterdam), pp. 1822–1823, IEEE, Oct 31- Nov 3 1996.

[36] R. Parker, E. Gatzke, and F. Doye III, "Advanced model predictive control (MPC) for type I diabetic patient blood glucose control," in *Proceedings of the American Control Conference, 2000*, vol. 5, (Chicago, IL), pp. 3483–3487, IEEE, June 28 - 30 2000.

[37] L. Magni, D. Raimondo, L. Bossi, C. Dalla Man, G. De Nicolao, B. Kovatchev, and C. Cobelli, "Artificial pancreas: Closed-loop control of glucose variability in diabetes: Model predictive control of type 1 diabetes: An in silico trial," *Journal of Diabetes Science and Technology (Online)*, vol. 1, no. 6, p. 804, 2007.

[38] C. Ellingsen, E. Dassau, H. Zisser, B. Grosman, M. Percival, L. Jo-vanovič, and F. Doyle III, "Safety constraints in an artificial pan-creatic $\beta$ cell: an implementation of model predictive control with insulin on board," *Journal of Diabetes Science and Technology (Online)*, vol. 3, no. 3, p. 536, 2009.

[39] L. Magni, C. Toffanin, C. Dalla Man, B. Kovatchev, C. Cobelli, and G. De Nicolao, "Model predictive control of type 1 diabetes added to conventional therapy," in *18th IFAC World Congress (IFAC 2011)*, (Milano (Italy)), August 18 - September 2 2011.

[40] L. Magni, M. Forgione, C. Toffanin, C. Dalla Man, B. Kovatchev, G. De Nicolao, and C. Cobelli, "Artificial pancreas systems: Run-to-run tuning of model predictive control for type 1 diabetes subjects: In silico trial," *Journal of Diabetes Science and Technology (Online)*, vol. 3, no. 5, p. 1091, 2009.

[41] D. Campos-Delgado, M. Hernandez-Ordonez, R. Femat, and A. Gordillo-Moscoso, "Fuzzy-based controller for glucose regula-tion in type-1 diabetic patients by subcutaneous route," *Biomedical Engineering, IEEE Transactions on*, vol. 53, no. 11, pp. 2201–2210, 2006.

[42] F. Campos-Cornejo, D. Campos-Delgado, E. Dassau, H. Zisser, L. Jovanovic, and F. Doyle, "Adaptive control algorithm for a rapid and slow acting insulin therapy following run-to-run methodology," in *American Control Conference (ACC 2010)*, (Baltimore, Maryland), pp. 2009–2014, IEEE, June 30 - July 2 2010.

[43] J. Bondia, E. Dassau, H. Zisser, R. Calm, J. Vehí, L. Jovanovič, and F. Doyle III, "Coordinated basal–bolus infusion for tighter postprandial glucose control in insulin pump therapy," *Journal of Diabetes Science and Technology (Online)*, vol. 3, no. 1, p. 89, 2009.

[44] H. Kirchsteiger, L. Del Re, E. Renard, and M. Mayrhofer, "Robust-ness properties of optimal insulin bolus administrations for type 1 diabetes," in *American Control Conference (ACC 2009)*, (St. Louis, Missouri), pp. 2284–2289, IEEE, June 10 - 12 2009.

[45] C. Dalla Man, D. Raimondo, R. Rizza, and C. Cobelli, "Gim, simulation software of meal glucose-insulin model," *J Diabetes Sci Technol.*, vol. 1, no. 3, pp. 323–330, 2007.

[46] C. Dalla Man, R. Rizza, and C. Cobelli, "Meal simulation model of glucose-insulin system," *Biomedical Engineering, IEEE Transactions on*, vol. 54, no. 10, pp. 1740–1749, 2007.

[47] MATLAB, *version 7.12.0 (R2011a)*. Natick, Massachusetts: The MathWorks Inc., 2011.

[48] C. Dalla Man, M. Camilleri, and C. Cobelli, "A system model of oral glucose absorption: Validation on gold standard data.," *Biomedical Engineering, IEEE Transactions on*, vol. 53, no. 12, 2006.

[49] L. Ljung and MathWorks, Inc, "Matlab: System identification toolbox," 2011. MathWorks.

[50] M. Cescon, "Linear modeling and prediction in diabetes physiology," Licentiate Thesis 3250, Department of Automatic Control, Lund University, Lund, Sweden, June 2011.

[51] F. Ståhl, "Diabetes mellitus glucose prediction by linear and bayesian ensemble modeling," Licentiate Thesis Licencitate Thesis 3255, Department of Automatic Control, Lund University, Sweden, Dec. 2012.

[52] T. Gross, D. Kayne, A. King, C. Rother, and S. Juth, "A bolus calculator is an effective means of controlling postprandial glycemia in patients on insulin pump therapy," *Diabetes Technology and Therapeutics*, vol. 5, no. 3, pp. 365–369, 2003.

[53] K. Åström and B. Wittenmark, *Computer-controlled systems: theory and design*. Upper Saddle River, New Jersey: Prentice Hall, 1997.

[54] H. Trogmann, H. Kirchsteiger, and H. del Re, "Hybrid control of type 1 diabetes bolus therapy," in *49th IEEE Conference on Decision and Control (CDC 2010)*, (Atlanta, Georgia), pp. 4721 –4726, December 15-17 2010.

[55] H. Trogmann, H. Kirchsteiger, G. Castillo Estrada, and L. del Re, "Fast estimation of meal/insulin bolus effects in T1DM for in silico testing using hybrid approximation of physiological meal/insulin model," *Diabetes*, vol. 59, p. A136, 2010.

[56] The Mathworks, "Matlab optimization toolbox user's guide," 2011.

[57] F. Cameron, B. Bequette, D. Wilson, B. Buckingham, H. Lee, and G. Niemeyer, "A closed-loop artificial pancreas based on risk management," *Journal of Diabetes Science and Technology*, vol. 5, no. 2, p. 368, 2011.

[58] H. Kirchsteiger and L. del Re, "Reduced hypoglycemia risk in insulin bolus therapy using asymmetric cost functions," in *7th Asian Control Conference (ASCC 2009)*, (Hong Kong, China), pp. 751 –756, August 27-29 2009.

[59] P. Dua, F. Doyle, and E. Pistikopoulos, "Multi-objective blood glucose control for type 1 diabetes," in *Medical and Biological Engineering and Computing*, pp. 343 –352, june 2009.

[60] B. Kovatchev, M. Straume, D. Cox, and L. Farhy, "Risk analysis of blood glucose data: a quantitative approach to optimizing the control of insulin dependent diabetes," *Computational and Mathematical Methods in Medicine*, vol. 3, no. 1, pp. 1–10, 2000.

[61] S. Boyd and L. Vandenberghe, *Convex optimization.* Cambridge: Cambridge University Press, 2004.

[62] G. Shapira, O. Yodfat, A. HaCohen, P. Feigin, and R. Rubin, "Bolus guide: a novel insulin bolus dosing decision support tool based on selection of carbohydrate ranges," *Journal of Diabetes Science and Technology*, vol. 4, no. 4, p. 893, 2010.

[63] Y. Wang, E. Dassau, H. Zisser, L. Jovanovič, and F. Doyle III, "Automatic bolus and adaptive basal algorithm for the artificial pancreatic β-cell," *Diabetes Technology & Therapeutics*, vol. 12, no. 11, pp. 879–887, 2010.

[64] Diabetes Education Online, "Calculating insulin dose." `http://dtc.ucsf.edu/types-of-diabetes/type2/treatment-of-type-2-diabete%s/medications-and-therapies/type-2-insulin-rx/calculating-insulin-dose/`. Accessed 2012-11-15.

[65] "Bd diabetes: How to calculate your insulin sensitivity factor." `http://www.bd.com/us/diabetes/page.aspx?cat=7001&id=7605`. Accessed 2012-11-15.

[66] B. Kovatchev, W. Clarke, M. Breton, K. Brayman, and A. McCall, "Quantifying temporal glucose variability in diabetes via continuous glucose monitoring: mathematical methods and clinical application," *Diabetes Technology and Therapeutics*, vol. 7, no. 6, pp. 849–862, 2005.

[67] J. Pickup, "Insulin-pump therapy for type 1 diabetes mellitus," *New England Journal of Medicine*, vol. 366, no. 17, pp. 1616–1624, 2012.

[68] International Federation of Diabetes, "Guideline for management of postmeal glucose." `https://www.idf.org/guidelines/postmeal-glucose-2007`, 2007.

| Department of Automatic Control **Lund University** **Box 118** **SE-221 00 Lund Sweden** | *Document name* LICENTIATE THESIS | |
|---|---|---|
| | *Date of issue* March 2013 | |
| | *Document Number* ISRN LUTFD2/TFRT--3258--SE | |
| *Author(s)* Meike Stemmann | *Supervisor* Rolf Johansson, Anders Rantzer | |
| | *Sponsoring organisation* DIAdvisor (EU FP7) | |

*Title and subtitle*
Predictive Control of Diabetic Glycemia

*Abstract*

Diabetes Mellitus is a chronic disease, where the blood glucose concentration of the patient is elevated. This is either because of missing insulin production due to failure of the $\beta$-cells in the pancreas (Type 1) or because of reduced sensitivity of the cells in the body to insulin (Type 2). The therapy for Type 1 diabetic patients usually consists of insulin injections to substitute for the missing insulin. The decision about the amount of insulin to be taken has to be made by the patient, based on empirically developed rules of thumb.

To help the patient with this task, advanced mathematical algorithms were used in this thesis to determine intakes of insulin and counteracting glucose that can bring the blood glucose concentration back to normoglycemia. The focus in this work was to determine insulin and glucose intakes around mealtimes. These algorithms used optimization methods together with predictions of the blood glucose concentration and mathematical models describing the patient dynamics to determine the insulin and glucose doses. For evaluation, the control algorithms were tested in-silico using a virtual patient and are compared to a simple bolus calculator from the literature. The aim was to increase the time spent in the safe range of blood glucose values of $70 - 180$ [mg/dL].

*Key words*
predictive control, optimization, diabetes, biological systems

*Classification system and/or index terms (if any)*

*Supplementary bibliographical information*

| *ISSN and key title* 0280–5316 | | *ISBN* |
|---|---|---|
| *Language* English | *Number of pages* 98 | *Recipient's notes* |
| *Security classification* | | |